

Dissolved Organic Matter Impacts Nitrogen Fixation in the Arctic Ocean

Downloaded from: https://research.chalmers.se, 2026-11-24 14:22 UTC

Citation for the original published paper (version of record):
Zander, S., von Friesen, L., Fujiwara, A. et al (2026). Dissolved Organic Matter Impacts Nitrogen Fixation in the Arctic Ocean. Journal of Geophysical Research Biogeosciences, 131(10). http://dx.doi.org/10.1029/2026JG009929

N.B. When citing this work, cite the original published paper.

research.chalmers.se offers the possibility of retrieving research publications produced at Chalmers University of Technology. It covers all kind of research output: articles, dissertations, conference papers, reports etc. since 2004. research.chalmers.se is administrated and maintained by Chalmers Library

(article starts on next page)

Check for updates

JGR Biogeosciences

RESEARCH ARTICLE
10.1029/2026JG009929

Dissolved Organic Matter Impacts Nitrogen Fixation in the Arctic Ocean

Stine Zander[1], Lisa W. von Friesen[1,2], Amane Fujiwara[3], Urban Wünsch[4,5], Olivier Grosso[6], Mar Benavides[6,7], Takuhei Shiozaki[8], Colin A. Stedmon[4], and Lasse Riemann[1]

[1]Marine Biological Section, Department of Biology, University of Copenhagen, Helsingør, Denmark, [2]Now at Centre for Ecology and Evolution in Microbial Model Systems (EEMiS), Linnaeus University, Kalmar, Sweden, [3]Research Institute for Global Change, Japan Agency for Marine-Earth Science and Technology, Yokosuka, Japan, [4]National Institute of Aquatic Resources, Technical University of Denmark, Kgs. Lyngby, Denmark, [5]Now at Water Environment Technology Division, Architecture and Civil Engineering, Chalmers University of Technology, Gothenburg, Sweden, [6]Aix Marseille Univ, Université de Toulon, CNRS, IRD, MIO UM 110, Marseille, France, [7]National Oceanography Centre, Southampton, UK, [8]Atmosphere and Ocean Research Institute, The University of Tokyo, Kashiwa, Japan

Abstract Climate change-driven sea ice loss, increased primary production, and nitrogen depletion are reshaping biogeochemistry in the Arctic Ocean (AO). These changes potentially increase the importance of nitrogen fixation, the conversion of dinitrogen gas into bioavailable ammonium, carried out by microorganisms called diazotrophs. However, it remains unknown how climate change-driven changes, such as increased primary production and dissolved organic matter (DOM) from riverine discharge, will affect nitrogen fixation. We show nitrogen fixation rates along with the composition of present and transcriptionally active diazotroph communities across depths and contrasting hydrographic regimes in the Pacific sector of the AO. Nitrogen fixation was widespread but generally low (<1 nmol N L^{-1} d^{-1}). UCYN-A2, the nitroplast of a haptophyte, accounted for most of the present and expressed nitrogenase (*nifH*) genes. Experiments revealed that additions of labile DOM (monosaccharides, pyruvate, and acetate), filtered chlorophyll *a*-rich seawater (a proxy for autochthonous DOM) or 4-hydroxybenzoic acid (a proxy for terrestrial-derived DOM) stimulated nitrogen fixation at some stations, with responses largely depending on in situ conditions. UCYN-A1 and UCYN-A2 nitroplasts were the most responsive across DOM treatments, and elevated *nifH* gene transcription suggests the haptophyte-nitroplast symbioses can exploit diverse DOM sources. Our findings indicate that climate change, through its impact on DOM dynamics and primary production, may affect nitrogen fixation by particularly UCYN-A and thereby influence biogeochemistry and productivity in the AO.

Plain Language Summary As sea ice melts in the Arctic Ocean (AO), light will become more available in the upper water column, and nitrogen availability will likely limit phytoplankton production. This influences food web structure and the drawdown of CO_2. Nitrogen fixation, the microbial conversion of dinitrogen gas into bioavailable ammonium, carried out by microorganisms called diazotrophs, is widespread and important in the oceans, but information about this process in the AO is sparse. Here, we show that nitrogen fixation is widespread, but relatively low in the Pacific sector of the AO, and that it is mainly carried out by UCYN-A2, the nitrogen-fixing organelle of a phytoplankton. Our experiments revealed that DOM stimulated nitrogen fixation at some stations, with responses depending on in situ conditions. Climate will impact future dynamics of DOM, for instance, due to increased river runoff and elevated phytoplankton production. This may in turn affect nitrogen fixation and thereby influence nutrient cycling and productivity in the AO.

Key Points:

- Dissolved organic matter (DOM) can stimulate nitrogen fixation in the Arctic Ocean (AO)
- UCYN-A is the key diazotroph in the Pacific region of the AO
- Changes in DOM load due to climate change might affect future nitrogen fixation

Supporting Information:

Supporting Information may be found in the online version of this article.

Correspondence to:

L. Riemann,
lriemann@bio.ku.dk

Citation:

Zander, S., von Friesen, L. W., Fujiwara, A., Wünsch, U., Grosso, O., Benavides, M., et al. (2026). Dissolved organic matter impacts nitrogen fixation in the Arctic Ocean. *Journal of Geophysical Research: Biogeosciences*, *131*, e2026JG009929. https://doi.org/10.1029/2026JG009929

Received 9 APR 2026
Accepted 6 OCT 2026

Author Contributions:

Conceptualization: Stine Zander, Lisa W. von Friesen, Colin A. Stedmon, Lasse Riemann
Data curation: Stine Zander, Lisa W. von Friesen, Amane Fujiwara, Urban Wünsch, Olivier Grosso, Mar Benavides
Formal analysis: Stine Zander
Funding acquisition: Lisa W. von Friesen, Takuhei Shiozaki, Colin A. Stedmon, Lasse Riemann
Investigation: Stine Zander, Lisa W. von Friesen, Amane Fujiwara
Methodology: Stine Zander, Lisa W. von Friesen, Urban Wünsch
Project administration: Stine Zander, Lasse Riemann

© 2026 The Author(s). Journal of Geophysical Research: Biogeosciences published by Wiley Periodicals LLC on behalf of American Geophysical Union. This is an open access article under the terms of the Creative Commons Attribution License, which permits use, distribution and reproduction in any medium, provided the original work is properly cited.

1. Introduction

The Arctic Ocean (AO) is the smallest ocean on Earth, representing 3% and 1% of the combined ocean area and volume, respectively, but accounts for up to 14% of the total oceanic CO_2 sink (Bates & Mathis, 2009; Manizza et al., 2019). This flux is largely sustained by Arctic primary production, which is often limited by the availability of inorganic nitrogen (N) (Mills et al., 2018; Tremblay et al., 2015). Therefore, understanding N inputs to the AO is critical when predicting its future productivity, biogeochemistry, and carbon sequestration.

Dinitrogen (N_2) fixation, the biological reduction of N_2 gas to ammonium (NH_4^+), is carried out by specialized microorganisms termed "diazotrophs." In oligotrophic tropical and subtropical regions, the supply of fixed N by diazotrophs can account for up to 50% of new primary production (Capone et al., 2005). In the AO, N_2 fixation

Resources: Mar Benavides, Takuhei Shiozaki, Colin A. Stedmon, Lasse Riemann
Supervision: Lasse Riemann
Validation: Stine Zander, Lisa W. von Friesen, Colin A. Stedmon, Lasse Riemann
Visualization: Stine Zander
Writing – original draft: Stine Zander, Lasse Riemann
Writing – review & editing: Stine Zander, Lisa W. von Friesen, Amane Fujiwara, Urban Wünsch, Olivier Grosso, Mar Benavides, Takuhei Shiozaki, Colin A. Stedmon, Lasse Riemann

rates have been determined in several regions such as the Pacific inflow (Bering Strait; Shiozaki et al., 2017, 2018), Chukchi and Beaufort Seas (Harding et al., 2018; Sipler, Gong, et al., 2017), the Canadian Arctic Archipelago (Blais et al., 2012), the Atlantic inflow (Zander, von Friesen, Gonçalves-Araujo, et al., 2026), and the Eurasian Basins (von Friesen, Farnelid, et al., 2025). Hence, N_2 fixation is widespread, but the measurements are spatiotemporally sparse (von Friesen & Riemann, 2020). Still, the reported rates may significantly influence primary production and carbon dioxide sequestration, and affect the AO's regional biogeochemistry (Shiozaki et al., 2018; Sipler, Gong, et al., 2017).

The composition of diazotroph communities in the AO has mainly been examined based on the nitrogenase gene (*nifH*), a widely used biomarker for N_2 fixation (Zehr et al., 1998). In the Pacific sector of the AO, the diazotroph UCYN-A fixes N_2 (Harding et al., 2018), and both the UCYN-A1 and UCYN-A2 sublineages are predominant in the Bering (Harding et al., 2018; Shiozaki et al., 2017) and Chukchi (Shiozaki et al., 2018) Seas. UCYN-A was previously thought to be a cyanobacterial symbiont associated with a haptophyte host but is now considered a N_2 fixing organelle ("nitroplast") within the haptophyte *Braarudosphaera bigelowii* (Coale et al., 2024). Cyanobacteria and UCYN-A are usually rare in the Atlantic sector of the AO, where non-cyanobacterial diazotrophs (NCDs) dominate both diazotroph community composition (Blais et al., 2012; Fernández-Méndez et al., 2016; von Friesen et al., 2023; Zander, von Friesen, Gonçalves-Araujo, et al., 2026) and *nifH* gene expression (von Friesen, Farnelid, et al., 2025, von Friesen, Laber, et al., 2025). Importantly, cyanobacteria and NCDs have fundamentally different metabolisms, mainly photoautotrophs or heterotrophs, respectively (Bombar et al., 2016; Chakraborty et al., 2021; Coale et al., 2024; Turk-Kubo et al., 2022; Zehr & Capone, 2020); thus, their responses to future environmental perturbations in the AO will likely depend on the prevailing ecological drivers and the region in question. Most NCDs are thought to be heterotrophic, meaning their activity is expected to be regulated by DOM (Bombar et al., 2016; Turk-Kubo et al., 2022). For instance, DOM stimulated NCD activity in the Mediterranean Sea (Rahav et al., 2016) and the South Pacific Ocean (Benavides et al., 2016, 2022), and uptake of DOM by NCDs was documented in the North Pacific (Filella et al., 2025). Likewise, N_2 fixation was stimulated by dissolved organic carbon (DOC) amendment in the central AO, where NCDs predominate (von Friesen, Farnelid, et al., 2025). DOM availability may, however, also affect cyanobacterial diazotrophs. For example, DOM was identified as a limiting factor for N_2 fixation by both NCDs and cyanobacteria in the South Pacific Ocean (Benavides et al., 2015; Moisander et al., 2012). However, DOM can also stimulate cyanobacterial growth and *nifH* gene expression (Benavides et al., 2017, 2020; Bonnet et al., 2013; Filella et al., 2024). Finally, in a recent study, DOM uptake was documented for the UCYN-A nitroplast (Filella et al., 2025). Hence, DOM appears to be a driver not only for the putative heterotrophic NCDs, but also for photosynthesizing organisms, including the nitroplast–haptophyte symbiosis. The extent to which DOM regulates N_2 fixation in the AO is, however, unknown.

Due to its large watershed (Rudels & Carmack, 2022), the AO receives about 11% of the global river discharge and thereby large amounts of terrestrially dominated DOM and particulate organic matter (McClelland et al., 2012). This freshwater input is expected to increase (Terhaar et al., 2019), causing an elevated load of terrestrial DOM including lignin-derived compounds into the coastal and shelf regions of the AO (Kong et al., 2025; Mann et al., 2016). These predictions also include the Pacific AO sector where permafrost thawing, riverine discharge and coastal erosion are expected to continue to increase (Mathew et al., 2025). For a long time, terrestrial DOM supplied by Arctic rivers was thought to be not available for microbes (Amon & Meon, 2004; Opsahl et al., 1999; Tank et al., 2012). However, there is increasing evidence showing that up to 40% of terrestrial DOM is utilizable by Arctic microbes (Hansell et al., 2004; Holmes et al., 2008; Mann et al., 2012; Sipler, Kellogg, et al., 2017). In addition to allochthonous sources of DOM mentioned above, phytoplankton release autochthonous DOM (Baines & Pace, 1991). The Arctic is warming up to four times faster than the global average (Rantanen et al., 2022), which has led to a rapid decline in sea ice cover. Primary production in the AO increased by 57% between 1998 and 2018 (Lewis et al., 2020) and is expected to increase further as diminishing sea ice enhances light availability (Ardyna & Arrigo, 2020). This will likely increase the supply of bioavailable DOM released from phytoplankton (Baines & Pace, 1991). Hence, the increased river discharge and primary production will likely alter the quantity, characteristics, and distribution of DOM, but the effects on N_2 fixation are unknown. Understanding the relationship between DOM and N_2 fixation in the AO is therefore critical for the accuracy with which N_2 fixation in the future AO can be predicted.

Our study was conducted in the Pacific region of the AO, which is characterized by complex hydrography and encompasses water masses that differ in productivity and riverine influence. This region is therefore well-suited

21698961, 2026, 10, Downloaded from https://agupubs.onlinelibrary.wiley.com/doi/10.1029/2026JG009929 by Statens Beredning, Wiley Online Library on [30/10/2026]. See the Terms and Conditions (https://onlinelibrary.wiley.com/terms-and-conditions) on Wiley Online Library for rules of use; OA articles are governed by the applicable Creative Commons License

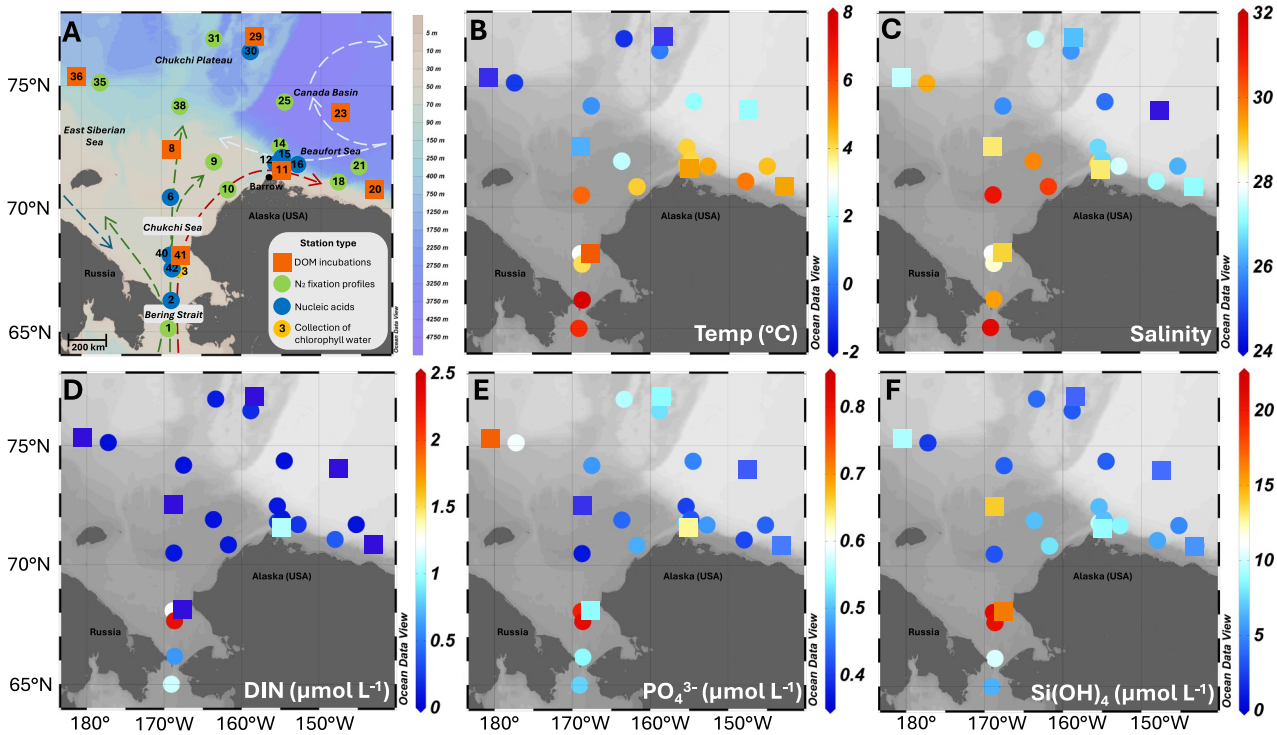


Figure 1. Sampled stations and ancillary data. (a) The sampled stations (numbers refer to station ID): dissolved organic matter experiments and 5 m N_2 fixation and primary production rates (orange), N_2 fixation and primary production depth profiles (green), nucleic acids only (blue), and collection of high chlorophyll *a* seawater from 16 m depth (station 3; yellow; Data Set S3). Water currents (modified from Rudels and Carmack (2022)) are shown with arrows: Siberian Coastal Current (blue), Anadyr Current (green), Alaskan Coastal Current (red), Beaufort Gyre (white), (b) temperature, (c) salinity, (d) dissolved inorganic nitrogen, (e) phosphate (PO_4^{3-}), and (f) silicate ($Si(OH)_4$) from 5 m depth. DOM-experiment stations are shown as squares, and all other stations as circles. Note that the *y*-axis have different ranges.

for testing the hypothesis that DOM stimulates diazotrophs and increases their N_2 fixation activity. We characterized DOM properties and concentrations and compared them with qualitative and quantitative data on diazotrophs under different environmental conditions. Further, we coupled this information to on-site manipulation experiments examining the influence of labile DOM, phytoplankton-derived DOM, and terrestrial DOM on N_2 fixation and diazotroph activity.

2. Materials and Methods

2.1. Study Region and Ancillary Data Collection

Samples were obtained onboard R/V *Mirai* from 4 September to 4 October 2023 (cruise number: MR23-06C) and targeted the diverse water masses associated with the Bering Strait, Chukchi Sea and Plateau, Alaskan Coast, Canada Basin, and the margin of the East Siberian Sea. In total, 25 stations (Figure 1a) were sampled for either *nifH* community composition and expression, N_2 fixation, or DOM addition experiments. *NifH* community composition and expression were examined at all stations, whereas N_2 fixation rate measurements and DOM addition experiments were carried out at selected stations. In general, *nifH* community composition, expression, and N_2 fixation rates were measured from 5, 20, 50, and 100 m depths at each station; however, at stations shallower than 50–100 m, the deepest depth sampled was 5 m above the bottom. Samples were obtained with Niskin bottles mounted on a rosette frame, and depth profiles of temperature and salinity were recorded with an SBE 911-plus CTD system (Sea-Bird Electronics, Bellevue, WA, USA). Nitrate (NO_3^-), nitrite (NO_2^-), ammonium (NH_4^+), silicate ($Si(OH)_4$), phosphate (PO_4^{3-}), and chlorophyll *a* (chl. *a*) concentrations at each depth were measured onboard using a QuAAtro 39-J system (BL TEC K.K., Japan) and a fluorometer (Turner, CA, USA), respectively. Collectively NO_3^-, NO_2^-, and NH_4^+ are referred to as dissolved inorganic nitrogen (DIN). In situ DOM fluorescence was measured using the CTD system with a Seapoint Ultraviolet Fluorometer (SUVF; Seapoint Sensors, NH, USA). Dissolved oxygen was measured using a RINKO III (JFE Advantech CO., Ltd., Hyogo, Japan) and corrected using the temperature and salinity sensor values. A detailed description of

21698961, 2026, 10, Downloaded from https://agupubs.onlinelibrary.wiley.com/doi/10.1029/2026JG009929 by Statens Beredning, Wiley Online Library on [30/10/2026]. See the Terms and Conditions (https://onlinelibrary.wiley.com/terms-and-conditions) on Wiley Online Library for rules of use; OA articles are governed by the applicable Creative Commons License

21698961, 2026, 10, Downloaded from https://agupubs.onlinelibrary.wiley.com/doi/10.1029/2026JG009929 by Statens Beredning, Wiley Online Library on [30/10/2026]. See the Terms and Conditions (https://onlinelibrary.wiley.com/terms-and-conditions) on Wiley Online Library for rules of use; OA articles are governed by the applicable Creative Commons License

ancillary data measurements is available in the cruise report (JAMSTEC, 2023). Samples for the determination of bacterial abundance were fixed with glutaraldehyde (0.5% final concentration, Sigma Aldrich, MA, USA), incubated at room temperature for 10 min, and frozen at −80°C until analysis. On land, samples were thawed, pre-filtered (30 μm), stained with SYBR Green I (0.1% final concentration, Invitrogen, MA, USA), and enumerated using a blue laser at 488 nm and green fluorescence and side scatter signatures (LE-SH800 flow cytometer, SONY Biotechnologies, CA, USA).

2.2. Dissolved Organic Matter Measurements

Samples for analyses of DOC, colored dissolved organic matter (CDOM), and fluorescent dissolved organic matter (FDOM) were filtered through 0.2 μm filters (Millipore Opticap XL filter capsule) into pre-combusted 40 mL glass vials that were stored in the dark at 4°C until analysis within 2 months of sampling. DOC samples were immediately acidified to pH 2 with phosphoric acid. DOC was quantified with high-temperature catalytic combustion (Shimadzu TOC-VCPH + ASI-V) by injection of 100 μL sample onto the catalyst up to seven times, and the average of the three most similar signal integration was calculated automatically. Column-specific calibrations were performed using acetanilide. The accuracy of the calibration was verified after every 8th sample using a combination of ultrapure water and two reference standards of 62 and 102 μM carbon, as well as a community reference material (University of Miami, Hansell Consensus Reference Material deep sea reference water, 41–45 μM carbon).

The optical properties of DOM were analyzed using a Horiba AquaLog spectrofluorometer in conjunction with a Shimadzu UV-1900i spectrophotometer. Absorbance measurements (CDOM) were performed in a 10 cm Suprasil-grade quartz cuvette (Hellma, Sigma-Aldrich, MA, USA) by scanning from 800 to 200 nm with 1 nm resolution at a 5 nm bandpass. The double-beam spectrophotometer was used with a single cuvette in the sample beam, leaving the reference beam empty. Daily blanks were measured in triplicate and subtracted from the sample measurements. Baseline offsets were subsequently corrected by subtracting the average absorbance above 600 nm. Absorbance slopes were calculated using the drEEM toolbox (v.2.25.10; https://zenodo.org/records/17182161) as described elsewhere (Helms et al., 2008; Stedmon & Markager, 2001). In particular, the slope ratios (Sr, the ratio of the slope of the absorption spectrum between 275 and 295 nm to that between 350 and 400 nm) were used as indicators of CDOM processing, with low values indicating a greater contribution of terrestrial material (allochthonous) that has not been exposed to photodegradation. Furthermore, a longer wavelength range exponential slope was calculated between 300 and 600 nm, with terrestrial material having values of approximately 18 μm^{-1} and fresh marine organic matter values of 10 μm^{-1} (Stedmon & Markager, 2001).

DOM fluorescence (FDOM) was measured at increasing excitation between 240 and 450 nm with 5 nm increments and emission detection between 211 and 618 nm at a 3.3 nm resolution in a 10 mm quartz cuvette (Suprasil grade, Hellma, Sigma-Aldrich, MA, USA). The integration time was 12 s. All processing of absorbance and fluorescence data was carried out in MATLAB R2025b using the drEEM toolbox. Inner-filter effects were corrected using the absorbance-based approach (Kothawala et al., 2013). Ultrapure water blanks were subtracted to minimize the extent of Rayleigh and Raman scatter, and the fluorescence signals were normalized by the area under the Raman peak at 350 nm (Ryder et al., 2017). Raman and Rayleigh scatter (first and second order) were removed without replacement, and data 20 nm below the calculated position of the first order Rayleigh peak were replaced with zero. A fluorescence ratio termed the freshness (or biological) index (FrI) was derived as the ratio of fluorescence at 380–430 nm, from an excitation wavelength at 310 nm, with high values indicating the presence of newly produced material (autochthonous) (Parlanti et al., 2000).

2.3. N_2 Fixation and Primary Production Rate Measurements

Measurements of N_2 fixation and primary production were performed as previously described (von Friesen, Farnelid, et al., 2025; Zander, von Friesen, Gonçalves-Araujo, et al., 2026). Briefly, seawater was collected from Niskin bottles into acid-washed polycarbonate bottles (2.3 L; Data Set S1), and $NaH^{13}CO_3$ (final concentration 100 μM, ≥98 atom%, Sigma Aldrich, MA, USA) was added to the bottles before being closed air-tight with septa caps. Bottles were then spiked with $^{15}N_2$ gas (1.3 mL L^{-1}; 99%, Cambridge Isotope Labs, MA, USA) and gently shaken for 15 min to enhance $^{15}N_2$ dissolution before removal of excess gas (Klawonn et al., 2015). Triplicate bottles were incubated for 24 hr in a transparent on-deck water bath with continuous flow-through of surface seawater. To mimic in situ light conditions, the bottles were shaded with either black nylon mesh or gray plastic

21698961, 2026, 10, Downloaded from https://agupubs.onlinelibrary.wiley.com/doi/10.1029/2026JG009929 by Statens Beredning, Wiley Online Library on [30/10/2026]. See the Terms and Conditions (https://onlinelibrary.wiley.com/terms-and-conditions) on Wiley Online Library for rules of use; OA articles are governed by the applicable Creative Commons License

bags according to measurements of photosynthetic active radiation from the CTD. To obtain the natural isotope ratios of $^{15}N/^{14}N$ and $^{13}C/^{12}C$ and concentrations of particulate organic carbon (POC) and nitrogen (PON), one separate reference bottle was filtered immediately onto glass fiber filters (pre-combusted GF75, nominal pore size 0.3 µm, Advantec™, Auburn, USA) from each sampled depth. This procedure was performed in triplicate at three stations to identify the standard deviation associated with our natural isotope ratio determination (<0.25%, Data Set S2). After incubation, duplicate 12 mL samples were collected in gas-tight exetainers (Labco, Lampeter, UK) and stored upside down submerged in seawater at 4°C, until analysis of the dissolved $^{15}N_2$ atom% by membrane inlet mass spectrometry (Kana et al., 1994). The remaining water was filtered onto glass fiber filters (as above) and stored at −20°C until later drying at 50°C for 24 hr. Lastly, POC and PON concentrations were measured using a coupled Elemental-Analyzer to Isotope-Ratio-Mass Spectrometer (EA-IRMS; Integra 2, SerCon Ltd, Chesire, UK). N_2 fixation rates were calculated using the template provided by White et al. (2020) (Data Set S1) with the limit of detection (LOD) calculated according to Gradoville et al. (2017). Rates below the LOD were defined as zero. Primary production rates (Data Set S2) were calculated according to Hama et al. (1993). Depth-integrated N_2 fixation and primary production rates were calculated for stations with measurements from multiple depths using trapezoidal integration, assuming linear interpolation between measured points. The potential contribution of N_2 fixation to primary production was estimated using the Redfield ratio (Redfield, 1934). In parallel, the in situ C:N ratios were included to account for potential differences in elemental stoichiometry (Martiny et al., 2013). Furthermore, the uncertainty in the estimated contributions was calculated using standard error propagation based on the standard deviations of triplicate N_2 fixation and primary production measurements, thereby, accounting for variability in both parameters.

2.4. Dissolved Organic Matter Experiments

To examine the influence of three different types of DOM on N_2 fixation rates, DOM amendment experiments were carried out at stations 8, 11, 20, 23, 29, 36, and 41 in 4.6 L bottle incubations. The overall aim was to test whether N_2 fixation was limited by DOM availability and evaluate responses to marine and terrestrial DOM sources that might change in the future AO (i.e., increased primary production and terrestrial DOM inputs). The experiments included triplicate control incubations supplied with $^{15}N_2$ gas and $NaH^{13}CO_3$ only, one control incubation with DOM amendment only (this was done for all three types of DOM), and triplicate DOM amendments with $^{15}N_2$ gas and $NaH^{13}CO_3$. It should be noted that the DOM amendments are simplified proxies rather than representative DOM types. The first treatment consisted of 10 µM dissolved organic carbon (termed "DOC" treatment) containing semi-labile monosaccharides typically found in Arctic summer waters (35.1% glucose, 27.1% mannose, 1.7% galacturonic acid, 8.6% rhamnose, 7.5% arabinose; von Jackowski et al., 2020) supplemented with 10% pyruvate and 10% acetate, as described in von Friesen, Farnelid, et al. (2025). The second amendment consisted of pre-filtered high chl. *a* water (termed "CHL" treatment) mixed 50:50 with sample water. For this treatment, 60 L of seawater was collected from the chl. *a* maximum (1.35 µg L^{-1}; 16 m depth) at station 3 (Figure 1a; Table S1 in Supporting Information S1; Data Set S3), which had high chl. *a* concentration compared to nearby stations. The seawater was 0.2 µm filtered (Opticap XL filter capsule, Millipore) and stored in the dark at 4°C until use. To account for the sample dilution of the CHL treatment, the measured N_2 fixation rates were doubled (Data Set S1). DOC concentrations and bacterial abundance were measured prior to filtration, after filtration, and immediately before being used in incubations (Table S1 in Supporting Information S1). The third amendment consisted of 10 µM 4-hydroxybenzoic acid (Sigma Aldrich, MA, USA), a model lignin-derived phenolic compound (termed "LIG" treatment) (Kuzyk et al., 2008). Some marine bacteria can degrade this compound and use it as their carbon source (Lu et al., 2020, 2022), and it is found in the AO (Grieman et al., 2018). After the addition of DOM compounds, bottles were treated and incubated as described above. After the 24 hr, 700 mL from each set of triplicate bottles was pooled and filtered on 0.22 µm Sterivex filters (Millipore, MA, USA) for *nifH* gene expression analysis (see below), while the rest was filtered for EA-IRMS (kept in triplicate).

2.5. Nucleic Acids Extraction, *nifH* Amplification, and Sequencing

Nucleic acids were sampled from 5 m depth across all 25 stations, and additionally from 20, 50, and 100 m depths at 19 stations (Figure 1a; Data Set S3). Seawater (0.7–2.3 L) was immediately filtered for up to 30 min onto 0.22 µm Sterivex filters in dimmed light. Filters were preserved with 1 mL RNAlater (Ambion, CA, USA) and stored at −80°C until dual extraction of DNA and RNA (AllPrep DNA/RNA Mini kit, Qiagen Sciences, MD,

21698961, 2026, 10, Downloaded from https://agupubs.onlinelibrary.wiley.com/doi/10.1029/2026JG009929 by Statens Beredning, Wiley Online Library on [30/10/2026]. See the Terms and Conditions (https://onlinelibrary.wiley.com/terms-and-conditions) on Wiley Online Library for rules of use; OA articles are governed by the applicable Creative Commons License

USA). Prior to extractions, filters were removed from the Sterivex housing and thoroughly ground with a sterile metal pestle, with intermittent flash freezing in liquid nitrogen up to five times. Following extractions, DNA and RNA concentrations were quantified using a Qubit fluorometer (Thermo Fischer Scientific, MA, USA) with the dsDNA HS Assay Kit and RNA HS Assay Kit, respectively. Post extraction, DNA and RNA were stored at −20° and −80°C, respectively. Triplicate blank Sterivex filters were included as contamination controls, covering all steps from sampling to sequencing.

cDNA was synthesized from RNA using SuperScript™ IV (Invitrogen, MA, USA) in 10 µL reactions with 5 µL RNA (averaging 56.5 ± 41 ng per reaction) and nifH3 (see below) as a gene-specific primer. *nifH* amplicons were generated from DNA and cDNA in nested PCR reactions (Zehr & Turner, 2001) using MyTaq polymerase (MyTaq HS Mix, Meridian Bioscience, OH, USA). Each PCR reaction was 25 µL, containing 1X MyTaq polymerase, 1 µg μL^{-1} bovine serum albumin (BSA), and 5 mM $MgCl_2$. The outer reaction included 0.4 µM primers nifH3 (ATRTTRTTNGCNGCRTA) and nifH4 (TTYTAYGGNAARGGNGG) (Zani et al., 2000) and the inner reaction contained 0.4 µM primers nifH1 (TGYGAYCCNAARGCNGA) and nifH2 (ADNGCCATCATYTCNCC) (Zehr & McReynolds, 1989). Thermal cycling conditions consisted of an initial denaturation at 95°C (60 s) followed by 30 cycles at 95°C (15 s), 50/57°C (60 s), and 72°C (10 s), and a final step at 72°C (300 s) for outer/inner reactions. In outer reactions, 1 µL cDNA template was added, and the DNA concentration averaged 4.2 ± 4.0 ng per reaction. For inner reactions, 1 µL of the outer PCR product was used as the template. All RNA samples were checked for DNA contamination by adding RNA extract directly to the nested PCR runs, generating no visible amplification. Negative controls consisting of PCR-grade water were included for all runs, and three of these were sequenced. All PCR products were checked by agarose gel electrophoresis. Triplicate inner PCR products were pooled, purified (GeneClean Turbo, MP Biomedicals, CA, USA), and quantified (Qubit). Five ng pooled amplicons were indexed with 0.2 µM Illumina indexes (National Genomics Infrastructure, Uppsala, Sweden), 1X MyTaq HS Mix and 3.5 mM $MgCl_2$ in eight cycles at 94°C (30 s), 62°C (30 s), 72°C (30 s) starting and ending at 94°C (60 s) and 72°C (300 s), respectively. Lastly, indexed amplicons were purified (Agencourt AMPure XP beads, Beckman Coulter, CA, USA), quantified (Qubit), pooled in equimolar ratios, and sequenced using an Illumina MiSeq v3 platform (Geo Genetics Sequencing Core, University of Copenhagen, Denmark).

2.6. Sequence Analyses

Sequences were analyzed in RStudio (v.4.2.1) as in von Friesen et al. (2023), in brief: using the DADA2-pipeline (v. 1.26.0; Callahan et al., 2016) with read trimming at 240 (forward) and 170 (reverse). Non-*nifH* reads and *nifH* homologs were removed using steps 2, 4 and 5 of the NifMAP pipeline (v.1.0; Angel et al., 2018). Assignment of *nifH* phylogenetic clusters was done according to Frank et al. (2016) and *nifH* taxonomy was assigned using assignTaxonomy (DADA2-pipeline) and a *nifH* database (v. 2.0.5; Moynihan & Furbo Reeder, 2023). A total of 1872 amplicon sequence variants (ASVs) were generated from the 165 DNA and RNA samples, three negative controls, and three contamination controls. ASV taxonomy, counts, and environmental data were merged into one object using phyloseq (v.1.36.0; McMurdie & Holmes, 2013) and used for downstream analyses. There was an average of 29,109 reads per sample, and three samples containing <1,000 reads were discarded. Based on the negative and contamination controls, four contaminants (ASVs 885, 948, 978, and 1,196) were identified (decontam v.1.12.0; Davis et al., 2018) and removed from the dataset. The remaining reads in control samples were considered negligible due to their low counts (4, 107, and 231, respectively). All ASVs classified as "*Candidatus* Atelocyanobacterium" (UCYN-A) from the taxonomic pipeline were assigned to UCYN-A1 or UCYN-A2 based on nucleotide sequence similarity to reference genomes (Hagino et al., 2013; Zehr et al., 2008) using Nucleotide BLAST (blast.ncbi.nlm.nih.gov). ASVs with no assigned taxonomy according to the DADA2-pipeline were termed "NAs." To gain insight into their phylogeny, NAs among the top 20 most abundant ASVs (on genus level) across DNA, RNA, and DOM samples (post DOM incubation) were aligned with selected reference sequences using MAFFT (L-INS-I; Katoh & Standley, 2013). A maximum-likelihood tree with 100 bootstraps was then constructed in RaxML-GUI (v. 2.0.13; Edler et al., 2021). First, the ModelTest-ng was applied to find the optimal substitution model and rate heterogeneity settings for the tree (G4, gamma mean), and the final tree was visualized in iTOL (Letunic & Bork, 2021).

2.7. Quantification of UCYN-A1 and UCYN-A2 *nifH* Genes and Transcripts

NifH gene and transcript abundances (copies L^{-1} seawater) were determined by quantitative polymerase chain reaction (qPCR) for two of the dominant diazotrophs identified by sequencing (UCYN-A1 and UCYN-A2).

21698961, 2026, 10, Downloaded from https://agupubs.onlinelibrary.wiley.com/doi/10.1029/2026JG009929 by Statens Beredning, Wiley Online Library on [30/10/2026]. See the Terms and Conditions (https://onlinelibrary.wiley.com/terms-and-conditions) on Wiley Online Library for rules of use; OA articles are governed by the applicable Creative Commons License

While UCYN-A2 was quantified for all stations (165 samples), qPCR targeting UCYN-A1 was only performed for 10 stations (71 samples) where its relative abundance accounted for >10% of the *nifH* sequence reads at one sample depth or more. Samples were run in triplicate 13 µL reactions in 96-well plates on a QuantStudio™ 1 (Thermo Fischer Scientific, MA, USA) using specific primer-probe sets (Church et al., 2005; Thompson et al., 2014). Reactions consisted of 4.7 ± 1.5 ng DNA or 1 µL cDNA, 1X Taqman® Universal PCR Master Mix (Applied Biosystems), 0.5 µM forward and reverse primers, 0.2 µM probe, 0.1 µg μL^{-1} BSA, and PCR-grade water. Reactions were run at 50°C (120 s), 95°C (10 min), followed by 45 cycles at 95°C (30 s) and 60°C (60 s). For each run, duplicate dilutions (10^1–10^8 copies) of UCYN-A1/UCYN-A2 standards (synthesized at GENEWIZ, NJ, USA), one negative control (PCR-grade water), and duplicate inhibition controls (a standard concentration of 10^5 or 10^6 copies added to an environmental sample) were included. For all runs, no amplification took place in the negative control, and all inhibition controls displayed no inhibition of amplification caused by environmental samples. Assay efficiency averaged 93.4 ± 4.2% across all runs (Data Set S3). The LOD and limit of quantification were calculated for each sample according to Armbruster and Pry (2008). Samples with no amplification were set as 0 in downstream analyses. For $\log_{10}$ conversion, samples with zero copies L^{-1} were set as 1.

2.8. Data and Statistical Analyses

Statistical analyses were performed in RStudio (v.4.2.1), and data visualization was done with ggplot2 (v.3.4.0; Wickham, 2016), Ocean Data View (v.5.8.1; Schlitzer, 2023), and MicroViz (v.0.10.0; Barnett et al., 2021). To evaluate correlations between N_2 fixation and ancillary data, Spearman's rank and Kendall's tau correlations were used on z-scored data. Correlations between UCYN-A2 *nifH* gene/transcript copies L^{-1} and ancillary data were evaluated with Spearman's rank correlation on z-scored data. For correlations, all *p*-values were adjusted using the false discovery rate to account for multiple testing. To assess differences in DOM characteristics between 5 m samples from all stations, principal component analysis (PCA) was performed using the prcomp function on z-scored data from DOM measurements. The envfit function (999 permutations and Bonferroni correction) from the vegan package (v.2.6.2; Oksanen et al., 2022) was used on centered log ratio-transformed ASV count table data (across all ASVs) to evaluate potential drivers of community composition at 5 m depth. Redundancy analysis (RDA) was then used to evaluate the proportion of variation explained by selected environmental parameters, as indicated by the envfit results. To validate the final RDA model, the *anova.cca* and *vif.cca* (<4) functions were used. The final model was visualized with MicroViz (v.0.10.0; Barnett et al., 2021) for the top five genera. Significant differences in N_2 fixation rates between control samples and DOM treatments were assessed using one-way analysis of variance (ANOVA) followed by Tukey's HSD post hoc test. Assumptions of normality and homogeneity of variances were tested using the Shapiro-Wilk and Levene's tests, respectively. For all statistics, *p*-values <0.05 were considered statistically significant.

3. Results

3.1. Environmental Context and In Situ Dissolved Organic Matter

The main focus of our study was the seven DOM experiments carried out with surface water (5 m depth, Figure 1a). Ancillary data and rate measurements reported below are therefore from 5 m depth, unless otherwise stated. Data from all stations and depths are provided in Data Set S3.

The sampled region is influenced by the Bering Strait inflow carrying relatively warm and nutrient-rich water from the Pacific Ocean into the Chukchi Sea and western AO (Figure 1a). This low salinity water (<33; Woodgate et al., 2012) also contains freshwater and terrestrial DOM from the Yukon River and Alaskan Coastal Current (Spencer et al., 2009). Upon entering the AO, part of the inflow follows the Alaskan shelf break, and part flows northwards into the Chukchi sea where it can mix with waters from the Siberian shelf (Mathis et al., 2007), which have high DOM concentrations (Charette et al., 2020; Stedmon et al., 2021).The sampled stations showed large temperature variation (from −1.7 to 7.7°C) with higher temperatures in the Bering Strait, Chukchi Sea, and at Alaskan coastal stations (Figure 1b). Salinity ranged from 24.2 to 33.9 with higher salinity in the Bering Strait and Chukchi Sea (Figure 1c). DIN was below 0.5 µmol L^{-1} at 20 of 25 stations (Figure 1d) and the concentrations of PO_4^{3-} and $Si(OH)_4$ averaged 0.5 ± 0.1 and 7.9 ± 5.2 µmol L^{-1} across all stations, respectively (Figures 1e and 1f). Based on all measured DOM properties, samples with allochthonous (terrestrial origin) or autochthonous (phytoplankton origin) influence could be distinguished (Figure 2). Autochthonously dominated stations showed

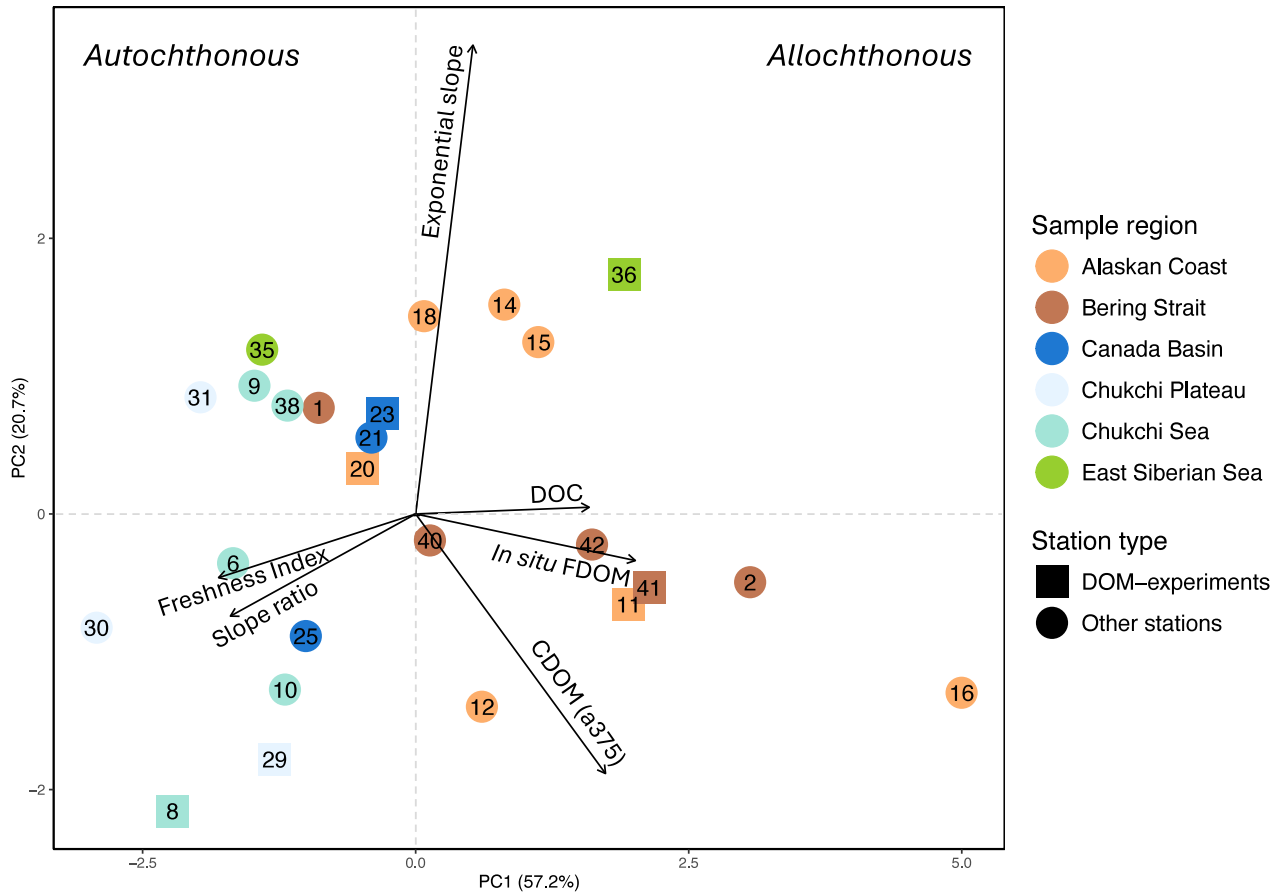


Figure 2. Dissolved organic matter (DOM) characteristics across stations. Principal component analysis of DOM measurements from all stations displayed as the first two principal components. Colors divide stations by sample region and DOM-experiment stations are presented as squares. DOM characteristics divide stations into autochthonous (marine originated DOM) or allochthonous (terrestrial originated DOM) based on the measured properties (see "DOM measurements" in methods).

higher values of FrI and Sr, and lower values of CDOM (a375) and exponential slope (see methods). The division was visible in a PCA model, where PC1 separated by DOM character (Figure 2). The FrI and DOC concentrations ranged from 0.70 to 1.0 and from 70.4 to 191 μmol L^{-1}, respectively (Figures 3a and 3b). Bacterial abundance ranged from 1.8×10^5 to 1.0×10^6 cells mL^{-1} and was generally lowest at northern stations (>74°N; Figure 3c). The chl. *a* concentration was generally low (<0.5 μg L^{-1}); however, it was elevated at a few coastal stations reaching 2.6 μg L^{-1} (Figure 3d).

3.2. N_2 Fixation and Primary Production In Situ

N_2 fixation rates in surface water (5 m) ranged from below the LOD to 2.34 nmol N L^{-1} d^{-1} (Figure 3e). In general, the rates were low (<1 nmol N L^{-1} d^{-1}; except the elevated rate of 2.34 nmol N L^{-1} d^{-1} at station 20), and eight measurements out of 17 were below the LOD. In total, 43 N_2 fixation rate measurements were carried out across all stations and depths, of which 17 were below LOD (Data Set S1). N_2 fixation rates above LOD ranged from 0.03 (station 21 at 100 m) to 2.34 nmol N L^{-1} d^{-1} (station 20 at 5 m) and averaged 0.44 ± 0.50 nmol N L^{-1} d^{-1}. Depth-integrated rates (down to 100 m) ranged from 0 to 23.6 μmol N m^{-2} d^{-1} (Table 1). No correlations between ancillary data and N_2 fixation rates were found (Table S2 in Supporting Information S1). Primary production at 5 m ranged from 22 to 3270 nmol C L^{-1} d^{-1} and appeared lowest at the northern stations (>74°N; Figure 3d). Depth-integrated primary production rates ranged from 79 to 661 mg C m^{-2} d^{-1} (Table 1). The potential contribution of N_2 fixation to primary production (based on the amount of new nitrogen added to the system and theoretically becoming available for primary producers) was generally below 1% but with values as high as 7% and 16% at 5 m and at depth 72.6 m, respectively (Table S3 in Supporting Information S1).

21698961, 2026, 10, Downloaded from https://agupubs.onlinelibrary.wiley.com/doi/10.1029/2026JG009929 by Statens Beredning, Wiley Online Library on [30/10/2026]. See the Terms and Conditions (https://onlinelibrary.wiley.com/terms-and-conditions) on Wiley Online Library for rules of use; OA articles are governed by the applicable Creative Commons License

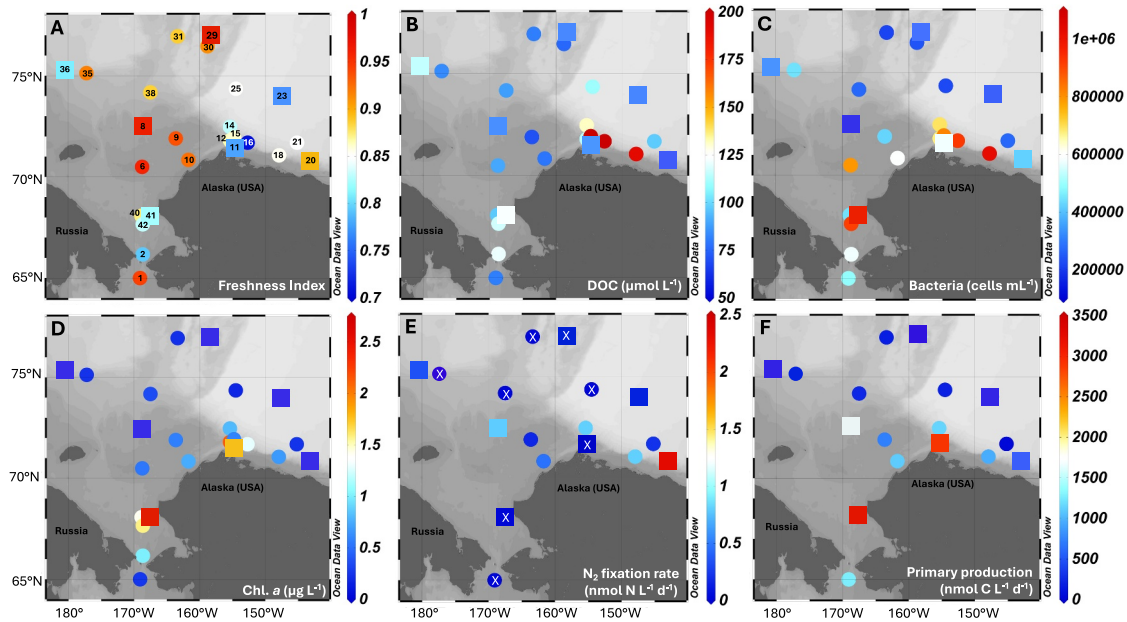


Figure 3. (a) Freshness Index, (b) dissolved organic carbon concentrations (µmol L^{-1}), (c) bacterial abundance (cells mL^{-1}), (d) chlorophyll *a* concentration (Chl. *a*; µg L^{-1}), (e) N_2 fixation rates (nmol N L^{-1} d^{-1}), and (f) primary production (nmol C L^{-1} d^{-1}). Numbers in (a) indicate station IDs. For N_2 fixation rates, rates below the limit of detection are marked with X. DOM-experiment stations are shown as squares, and all other stations as circles. All data are from 5 m depth. Note the different ranges on the *y*-axis.

3.3. Present and Active Diazotrophs

Amplification of the *nifH* gene was successful for all DNA and RNA samples, except for RNA samples from stations 15 and 40 (Figure S1 in Supporting Information S1). Across all in situ samples (i.e., excluding DOM-experiments), the most abundant diazotroph was UCYN-A2, accounting for 32% and 74% of the reads obtained from DNA and RNA samples, respectively (Figure S1 in Supporting Information S1). UCYN-A1 was the second most abundant, accounting for 5% and 13% of reads from DNA and RNA samples, respectively. A substantial proportion of ASVs (29% of all reads) lacked genus-level taxonomic assignment (NAs), although, at the class level, this proportion was 11% (data not shown). These ASVs mainly belonged to classes Deltaproteobacteria and Gammaproteobacteria and were placed in *nifH* subclusters 1A, 1G, 1K, 3E, and 3N (Figure S2 in Supporting Information S1), displaying variable similarities (82%–100%) to bacteria previously found in the AO (Fernández-

Table 1
Depth-Integrated N_2 Fixation and Primary Production Rates at Stations Where Data Were Available From Several Depths (Data Sets S1 and S2)

Station ID	Sample date (dd.mm.yyyy)	Sample region	Depths	N_2 fixation rate (µmol N m^{-2} d^{-1})	Primary production (mg C m^{-2} d^{-1})
1	07.09.2023	Bering Strait	5, 20, 40	16.8	397.5
9	10.09.2023	Chukchi Sea	5, 20, 35	6.8	314.3
10	11.09.2023	Chukchi Sea	5, 20, 39	10.3	332.0
14	13.09.2023	Alaskan Coast	5, 20, 50, 100	16.9	261.7
18	15.09.2023	Alaskan Coast	5, 20, 50, 100	23.6	197.0
21	17.09.2023	Canada Basin	5, 20, 50, 100	9.0	171.1
25	20.09.2023	Canada Basin	5, 20, 50, 100	10.5	79.2
31	22.09.2023	Chukchi Plateau	5, 20, 50	4.3	661.1
35	26.09.2023	East Siberian Sea	5, 20, 50, 100	0	138.8
38	28.09.2023	Chukchi Sea	5, 20, 50, 100	0	146.3

Note. Rates were integrated to the deepest depth sampled at each station.

21698961, 2026, 10, Downloaded from https://agupubs.onlinelibrary.wiley.com/doi/10.1029/2026JG009929 by Statens Beredning, Wiley Online Library on [30/10/2026]. See the Terms and Conditions (https://onlinelibrary.wiley.com/terms-and-conditions) on Wiley Online Library for rules of use; OA articles are governed by the applicable Creative Commons License

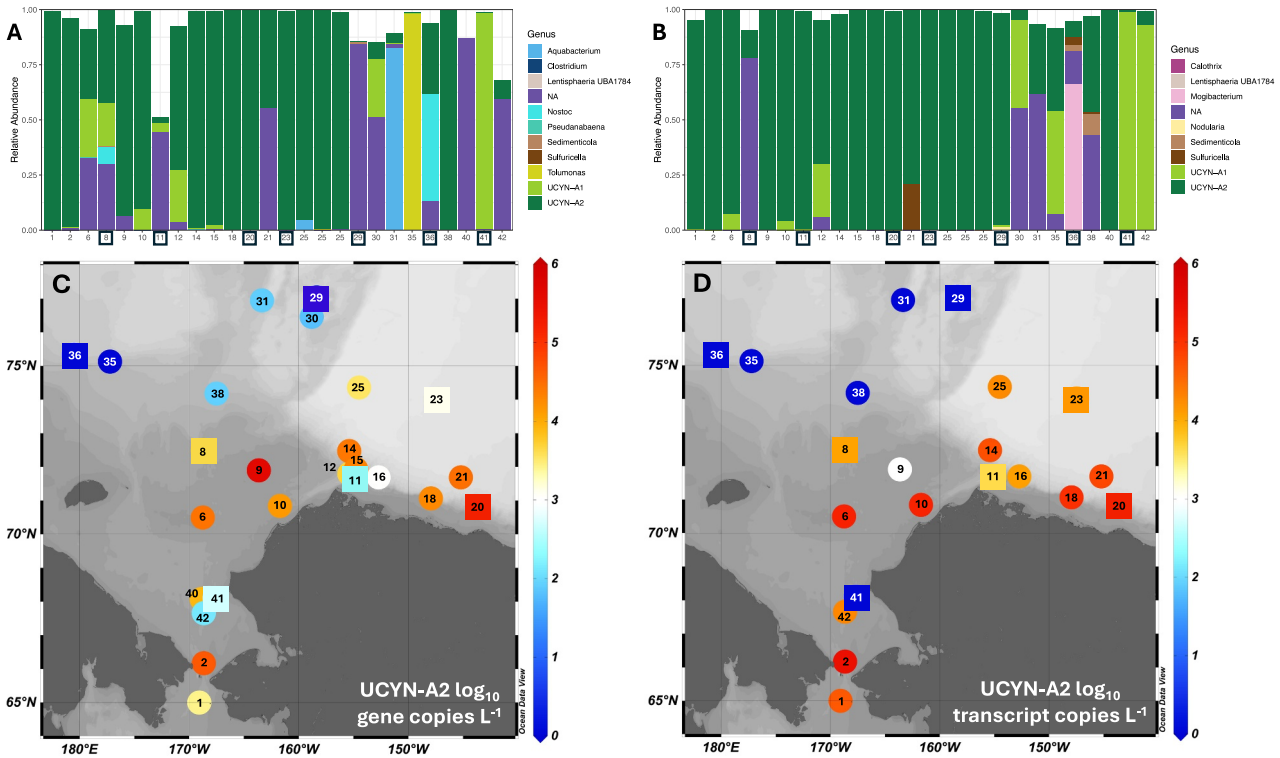


Figure 4. Diazotroph community composition and UCYN-A2 *nifH* transcriptional activity. The upper panels show the community composition (a) and *nifH* expression (b) for the top 100 amplicon sequence variants in the *nifH* amplicon sequencing data. Genus "NA": taxonomy not assigned from sequence analysis. The lower panels show UCYN-A2 gene copies L^{-1} (log_{10}) (c) and UCYN-A2 transcript copies L^{-1} (log_{10}) (d). DOM-experiment stations are shown as squares (in all panels) and all other stations as circles (panels c and d). Numbers indicate station IDs.

Méndez et al., 2016; Shiozaki et al., 2018; von Friesen, Farnelid, et al., 2025). Overall, the *nifH* gene Clusters I and III accounted for 83.5% and 16.1% of all reads, respectively (data not shown).

In the 5 m samples, UCYN-A2 dominated community composition and expression (>50% reads) across 14 and 18 samples from the 25 stations, respectively (Figures 4a and 4b). This included expression in seven samples where N_2 fixation was detected (stations 9, 10, 14, 18, 20, 21, and 23; Figures 3c and 4b). *NifH* transcripts were mainly observed for UCYN-A2 and UCYN-A1, however, also for a few NCDs, including the genera *Sedimenticola, Sulfuricella*, and *Mogibacterium*. The redundancy analysis indicated that the diazotroph community composition across 5 m samples could be explained by silicate, DIN, and chl. *a* up to 18% (RDA, $F = 1.9$, $p = 0.03$; Figure S3 in Supporting Information S1).

In the qPCR data, UCYN-A2 *nifH* gene and transcript abundance (log_{10} copies L^{-1}) at 5 m ranged from 0 to 5.7 and 0 to 6.0, respectively, with the highest concentrations mainly found in the Bering Strait, Chukchi Sea, and the Alaskan coastal stations (Figures 4c and 4d). Transcript and gene abundances generally decreased with depth but remained detectable down to 100 m (Figure S4 in Supporting Information S1). Across all sampled depths, UCYN-A2 *nifH* gene abundance was positively correlated ($p < 0.001$; Table S4 in Supporting Information S1), and gene ($p < 0.001$) and transcript ($p < 0.001$) abundance correlated positively with N_2 fixation (Table S2 in Supporting Information S1). Furthermore, UCYN-A2 gene abundance was positively correlated with primary production ($p < 0.05$), chl. *a* ($p < 0.05$), bacterial abundance ($p < 0.001$), and temperature ($p < 0.001$), whereas negative correlations were found with depth ($p < 0.05$) and phosphate ($p < 0.05$) (Table S4 in Supporting Information S1). Correlation analyses were also carried out exclusively for 5 m samples, revealing positive correlations of UCYN-A2 gene abundance with N_2 fixation ($p < 0.05$) and temperature ($p < 0.01$), and negative correlations with phosphate ($p < 0.01$) and oxygen ($p < 0.05$) (Tables S2 and S4 in Supporting Information S1). For transcript abundance, positive correlations were found with depth ($p < 0.05$), temperature ($p < 0.001$) and bacterial abundance ($p < 0.01$) and a negative correlation to phosphate ($p < 0.01$) across all depths, respectively (Table S4

21698961, 2026, 10, Downloaded from https://agupubs.onlinelibrary.wiley.com/doi/10.1029/2026JG009929 by Statens Beredning, Wiley Online Library on [30/10/2026]. See the Terms and Conditions (https://onlinelibrary.wiley.com/terms-and-conditions) on Wiley Online Library for rules of use; OA articles are governed by the applicable Creative Commons License

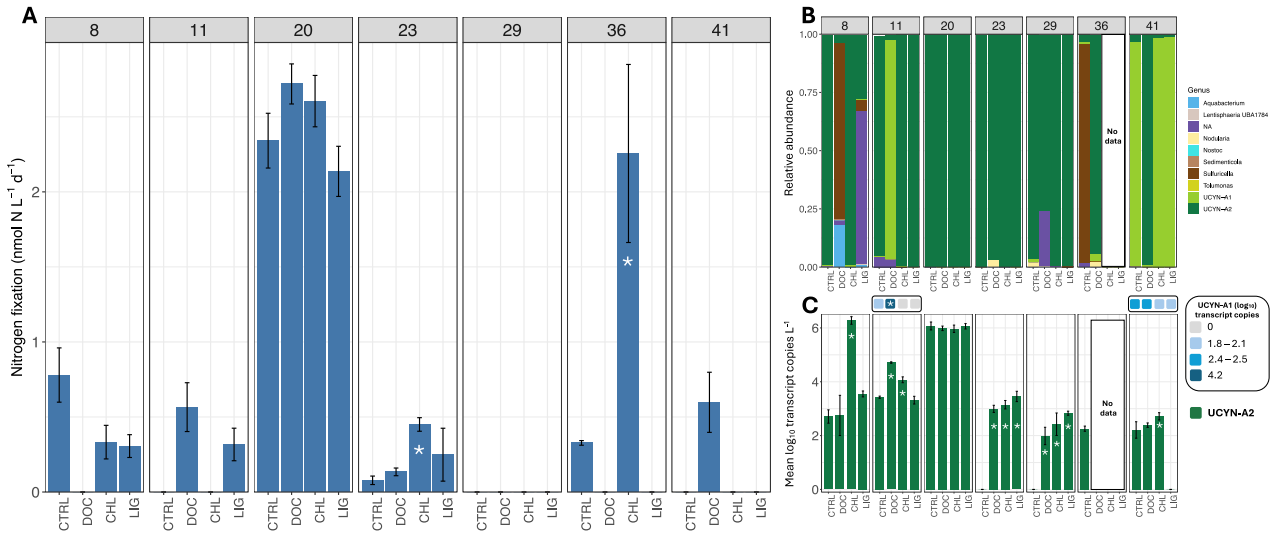


Figure 5. Results from dissolved organic matter (DOM) experiments. (a) N_2 fixation rates across triplicate incubations with error bars presenting the standard deviation, (b) composition of *nifH* transcripts upon termination of the incubation (T24) based on the top 100 amplicon sequence variants (amplicon sequence variants, accounting for 99.4% of all reads), and (c) *nifH* transcript copies ($\log_{10}$) L^{-1} for UCYN-A2 and UCYN-A1 at T24 assessed by quantitative PCR. Note that UCYN-A1 was quantified only at a subset of the stations (see methods). Error bars represent the standard deviation from triplicate technical measurements. Asterisks indicate whether the treatment was significantly higher than the control (tested with one-way analysis of variance). CTRL: control, DOC: labile DOM (single carbohydrates, pyruvate, acetate), CHL: chlorophyll-derived DOM (filtered seawater from a station rich in chl *a*), LIG: 4-hydroxybenzoic acid (a model lignin-derived phenolic compound).

in Supporting Information S1). At 5 m, transcript abundance correlated positively with temperature ($p < 0.01$) and negatively with oxygen ($p < 0.01$).

UCYN-A1 was quantified by qPCR for the 10 stations where it was found prominent among *nifH* sequence reads. Amplification occurred in 13 of 63 samples, all from 5 or 20 m, with *nifH* gene and transcript abundances reaching 10^3–10^4 copies L^{-1} (Figure S5 in Supporting Information S1).

3.4. Dissolved Organic Matter Experiments

DOM-experiments were carried out at seven selected stations representing water masses with contrasting conditions (Figure 1a). They differed in for example temperature (−1.3 to 5.8°C), chl. *a* concentration (0.13–2.6 µg L^{-1}), and bacterial abundance (1.9×10^5 to 1.0×10^6 cells mL^{-1}) (Figures 1b, 3c, and 3d; Data Set S3). The stations showed pronounced variation in DOM characteristics (Figure 2), also seen in the FrI (0.79–1.0; Figure 3a) and DOC (72.2–122.3 µmol L^{-1}; Figure 3b). From the PCA based on all DOM parameters, predominant DOM character at stations 11, 36, and 41 was allochthonous, and at stations 8, 20, 23, and 29 was autochthonous (Figure 2).

N_2 fixation was measured by $^{15}N_2$ incorporation over a 24 hr incubation period. After the incubation with DOM additions, samples were taken for identifying the *nifH* expressing organisms (cDNA amplicon sequencing) and for quantifying *nifH* gene transcripts (cDNA) of UCYN-A2 and UCYN-A1. N_2 fixation rates in the control incubations (no DOM added) were below LOD at three stations (11, 29 and 41) and control rates above LOD ranged from 0.08 to 2.34 nmol N L^{-1} d^{-1} (Figure 5a). UCYN-A2 and UCYN-A1 dominated the *nifH* gene expression (>50% relative abundance) in 23 of the 26 experimental samples, but expression by NCDs (the genera *Aquabacterium* and *Sulfuricella*, and NA) was occasionally prevalent (Figure 5b).

At stations 11 (Alaskan Coast) and 41 (Bering Strait), the control N_2 fixation rate was below LOD, but the DOC and LIG treatments displayed elevated rates (although not statistically significant). Interestingly, the DOC treatment at station 11 (Alaskan Coast) also showed increased transcript abundance for both UCYN-A1 (ANOVA, $F(3, 8) = 675.5$, $p < 0.001$) and UCYN-A2 (ANOVA, $F(3, 8) = 144.5$, $p < 0.001$) compared with the control. At station 36 (East Siberian Sea), N_2 fixation in the CHL treatment was higher than the control (ANOVA, $F(3, 8) = 12.27$, $p < 0.01$), but unfortunately, the RNA from this sample was not amplifiable by PCR or qPCR. At station 23 (Canada Basin), N_2 fixation in the CHL treatment was stimulated relative to the control

21698961, 2026, 10, Downloaded from https://agupubs.onlinelibrary.wiley.com/doi/10.1029/2026JG009929 by Statens Beredning, Wiley Online Library on [30/10/2026]. See the Terms and Conditions (https://onlinelibrary.wiley.com/terms-and-conditions) on Wiley Online Library for rules of use; OA articles are governed by the applicable Creative Commons License

21698961, 2026, 10, Downloaded from https://agupubs.onlinelibrary.wiley.com/doi/10.1029/2026JG009929 by Statens Beredning, Wiley Online Library on [30/10/2026]. See the Terms and Conditions (https://onlinelibrary.wiley.com/terms-and-conditions) on Wiley Online Library for rules of use; OA articles are governed by the applicable Creative Commons License

(ANOVA, F(3, 8) = 48.6, $p < 0.01$), and UCYN-A2 transcript abundance was increased (ANOVA, F(3, 8) = 370.2, $p < 0.001$). At station 23 (Canada Basin), the UCYN-A2 transcript abundance was also stimulated in the DOC (ANOVA, F(3, 8) = 370.2, $p < 0.001$) and LIG treatments (ANOVA, F(3, 8) = 370.2, $p < 0.001$). Elevated N_2 fixation was also seen at station 23 (Canada Basin), but this was not statistically supported. At stations 8 (Chukchi Sea) and 20 (Alaskan Coast), none of the DOM-treatments stimulated N_2 fixation relative to the control, but increased UCYN-A2 transcript abundance was seen in the CHL treatment at station 8 (ANOVA, F (3, 8) = 52.6, $p < 0.05$). At station 29 (Chukchi Plateau), N_2 fixation was always below LOD, but UCYN-A2 transcript abundance was elevated in all treatments (ANOVA, F(3, 8) = 62.2, $p < 0.001$ for all).

4. Discussion

Our study in the hydrographically complex Pacific AO shows that N_2 fixation was locally stimulated by the addition of labile DOC or filtered seawater from a chl. *a* maximum, but less so by the addition of the model lignin-derivative phenolic 4-hydroxybenzoic acid. Strikingly, UCYN-A2 showed the highest stimulation in *nifH* gene transcription in response to the experimental treatments.

Our sampling encompassed differences in DOM from high influence of terrestrial material in the Bering inflow (stations 2, 40, 41, 42) and downstream off the coast from Utqiagvik (Barrow, stations 11, 12, 14, 15, 16; Figure 1a) where DOM in surface waters had a low freshness index and high DOC concentrations (Figure 3). This links well with earlier studies in the same region that could trace a terrestrial signal along the Alaskan coast from the Pacific Ocean (Dainard & Guéguen, 2013). Over the Chukchi shelf, the DOM signature was different. These waters are shallow and productive, and sediments impart a clear biogeochemical signature, which can be exported into the Beaufort Sea (Mathis et al., 2007). This signal was also apparent in the DOM characteristics with a more autochthonous marine DOM signal, which fits with earlier findings (Dainard & Guéguen, 2013; Stedmon et al., 2011). In sub-surface waters, the properties of DOM can often be used as a tracer of water mass origin in the Arctic, with cold temperatures, a high degree of stratification and ice cover combined limiting alterations to DOM character (Stedmon et al., 2021). However, in late summer surface waters (<50 m), the signature is influenced by sea ice melt, exposure to photodegradation and contribution from phytoplankton, which causes DOM properties to vary more widely. This can in part explain the lack of clear correlations to N_2 fixation measurements.

4.1. Are N_2 Fixation Rates and UCYN-A2 Stimulated by DOM?

We carried out on-site manipulation experiments examining the influence of labile (a defined mixture monosaccharides and pyruvate and acetate), natural chlorophyll-derived (filtered and diluted water from a chl *a* maximum site), and a single model lignin-derived phenolic compound (to mimic terrestrial DOM) on N_2 fixation. It should be noted that these amendments are simplified proxies of representative DOM types. Hence, the experiments cannot be generalized to "marine DOM" or "terrestrial DOM" in a broad sense. The measurements integrate $^{15}N_2$ uptake over 24 hr, but the *nifH* gene expression data are not directly comparable because they originate from discrete sampling time points, and *nifH* gene expression is often temporally uncoupled from N_2 fixation (Severin et al., 2015). For instance, UCYN-A shows diel changes in *nifH* expression and may express *nifH* when not actively fixing N_2 (Gradoville et al., 2021), possibly explaining why nearly all samples were dominated by UCYN-A expression even when incubations were terminated at night (Table S5 in Supporting Information S1), where UCYN-A does not fix N_2 (Gradoville et al., 2021).

In the DOC treatment, samples were amended with a mixture of simple carbohydrates to determine whether N_2 fixation could be stimulated by labile DOC. While this is a common approach (Rahav et al., 2016; Benavides et al., 2017; von Friesen, Farnelid, et al., 2025), it should be noted that the selected compounds may not be accessible to all diazotrophs. For instance, glucose is accessible to most marine bacteria, but not all (Givati et al., 2024; Norris et al., 2021). Interestingly, DOC stimulated N_2 fixation at stations 11 (Alaskan Coast) and 41 (Bering Strait). These indicated the presence of predominantly allochthonous DOM (Figure 2), which is considered less available for microbial utilization (Grunert et al., 2021; Jørgensen et al., 2015). At both stations, UCYN-A1 and UCYN-A2 dominated the relative abundance (>95%) across all samples, and at station 11 both UCYN-A1 and UCYN-A2 transcript abundance were elevated compared to the controls. UCYN-A2 transcript abundance also increased in the DOC-treatment at stations 23 (Canada Basin) and 29 (Chukchi Plateau), classified as predominantly autochthonous, but displaying low primary production, bacterial abundance, and low in

21698961, 2026, 10, Downloaded from https://agupubs.onlinelibrary.wiley.com/doi/10.1029/2026JG009929 by Statens Beredning, Wiley Online Library on [30/10/2026]. See the Terms and Conditions (https://onlinelibrary.wiley.com/terms-and-conditions) on Wiley Online Library for rules of use; OA articles are governed by the applicable Creative Commons License

situ DOC. Taken together, labile DOC stimulated N_2 fixation and/or *nifH* gene transcription in waters where bioavailable DOM was conceivably in short supply.

Some marine prokaryotes (Raina et al., 2022) and diazotrophs (Hallstrøm, Raina, et al., 2022) exhibit chemotaxis toward phytoplankton-derived compounds, and it has been suggested that DOM leaking from primary producers stimulates N_2 fixation (Benavides et al., 2015; Filella et al., 2025; von Friesen, Farnelid, et al., 2025; Zander, von Friesen, Gonçalves-Araujo, et al., 2026). We therefore hypothesized that amendment with filtered water from a chl. *a* maximum (station 3; 1.35 μg chl. *a* L^{-1}) would stimulate N_2 fixation. Indeed, N_2 fixation was stimulated at stations 23 (Canada Basin) and 36 (East Siberian Sea) that were characterized by low temperatures (<2°C), primary production, chl. *a* concentration, and DOM freshness index (Figures 2 and 3). Moreover, the UCYN-A2 transcript abundance was increased at station 23 (Canada Basin), suggesting that N_2 fixation by UCYN-A2 was stimulated (RNA was unfortunately not available for station 36 (East Siberian Sea)). In fact, an increase in UCYN-A2 transcript abundance was observed in the CHL-treatment at five out of seven stations, suggesting that the UCYN-A2–*B. bigelowii* symbiosis can exploit phytoplankton-derived DOM. This falls in line with a recent study from the North Pacific Ocean, where UCYN-A uptake of ^{13}C-labeled DOM from phytoplankton cultures was documented by DNA stable isotope probing (Filella et al., 2025). Hence, DOM released from phytoplankton likely stimulates both N_2 fixation and transcript abundance in UCYN-A2, although this conclusion could be biased since the filtered water added to the CHL-treatment introduced bacteria (Table S1 in Supporting Information S1) that additionally could have served as prey for the phagotrophic *B. bigelowii* (Mak et al., 2024), hereby stimulating *nifH* gene expression and N_2 fixation by UCYN-A2.

Lignin-derived phenols serve as biomarkers for terrestrial DOM in the AO (Benner et al., 2005; Kaiser et al., 2017; Williford et al., 2022). We, therefore, used the lignin-derived phenol 4-hydroxybenzoic acid as a proxy for terrestrial DOM and applied it experimentally to elucidate the influence of terrestrial DOM on N_2 fixation (LIG treatment). Terrestrial DOM is partially available to bacterioplankton and may stimulate their activity (e.g., Traving et al., 2017), and select for specific bacterial taxa (e.g., Figueroa et al., 2021). Some marine bacteria can utilize 4-hydroxybenzoic acid (Lu et al., 2020), and some cultivated diazotrophs possess the genetic capacity for aromatic hydrocarbon metabolism (Bentzon-Tilia et al., 2015) and can grow with benzoic acid as the sole carbon source (Ngugi et al., 2007). Hence, we anticipated that benzoic acid would influence diazotrophs in our study.

Interestingly, we observed increased N_2 fixation in the LIG treatment at station 11 (Alaskan Coast), which was classified as predominantly allochthonous, and where N_2 fixation appeared to be constrained by in situ DOM conditions, as no measurable N_2 fixation was observed in the control incubation. Hence, under these conditions, N_2 fixation could be stimulated by bioavailable DOC (see above) as well as by our proxy for terrestrial DOM (a single phenolic model compound). Similarly, increased UCYN-A2 transcript abundance was observed in the LIG treatments at stations 23 (Canada Basin) and 29 (Chukchi Plateau), even though these offshore stations were characterized as autochthonous. This suggests that *B. bigelowii* may directly, or indirectly via intermediate bacterial degradation, utilize terrestrial DOM. However, it should be cautiously noted that it is not known whether the increased transcript abundance was caused by increased gene expression per cell or/and an increased number of cells, and the amendment was with a single phenolic model compound and not natural terrestrial DOM. At station 8 (Chukchi Sea), we observed a shift in *nifH* gene expression between the control sample and the LIG-treatment. Here, NCDs dominated the *nifH* expression with the highest abundance of ASVs in subcluster 1A (ASV 20 and 27; Figure S2 in Supporting Information S1) and one ASV in subcluster 3E (ASV 14). There is evidence that diverse Arctic Proteobacteria can utilize terrestrial DOM (Shiozaki et al., 2023; Sipler, Kellogg, et al., 2017), however, to what extent these include diazotrophs remains unknown. Overall, our experiments suggest that amendment with the lignin derived phenol 4-hydroxybenzoic acid can influence diazotrophs and N_2 fixation at contrasting sites, spanning from coastal to offshore waters, showing allochthonous or autochthonous DOM profiles.

Overall, our experiments illustrate that diazotrophs can respond to various types of DOM. However, it should be noted that responses were diverse and differed between stations, and N_2 fixation rates were commonly borderline to detection. Moreover, the amendments were simplified proxies for labile DOC (selected monosaccharides and pyruvate and acetate), DOM from a station rich in chl *a* (with implicit filtration and dilution effects) and terrestrial DOM (a single phenolic compound). Hence, the observed responses cannot be generalized to natural "marine" DOM or "terrestrial" DOM. The experiments show that occasionally diazotrophs or in some regions respond to

21698961, 2026, 10, Downloaded from https://agupubs.onlinelibrary.wiley.com/doi/10.1029/2026JG009929 by Statens Beredning, Wiley Online Library on [30/10/2026]. See the Terms and Conditions (https://onlinelibrary.wiley.com/terms-and-conditions) on Wiley Online Library for rules of use; OA articles are governed by the applicable Creative Commons License

these DOM amendments. While being important, additional research is needed to establish the spatio-temporal variability of these responses, and the response of diazotrophs to natural allochthonous and autochthonous DOM.

4.2. Key Diazotrophs and N_2 Fixation Across the Pacific Arctic Ocean

The diazotrophic community composition and *nifH* gene expression were strongly dominated by UCYN-A sublineages, especially UCYN-A2, for which both gene and transcript abundances were correlated with N_2 fixation. This suggests that the haptophyte *B. bigelowii* and its associated UCYN-A2 nitroplast is the key N_2-fixer in the Pacific sector of the AO, which aligns with previous work documenting its N_2 fixation activity in the Bering and Chukchi Seas (Harding et al., 2018). This is in contrast with the Atlantic sector of the AO, where NCDs prevail (Blais et al., 2012; Fernández-Méndez et al., 2016; von Friesen, Farnelid, et al., 2025; Zander, von Friesen, Gonçalves-Araujo, et al., 2026) and change to a UCYN-A dominated community only upon entering Atlantic waters to the south (von Friesen, Laber, et al., 2025). Similarly, in our study, UCYN-A2 gene and transcript abundances were positively correlated with temperature, and UCYN-A2 abundance was low and *nifH* transcripts were not detectable when reaching the colder waters of the Chukchi Plateau and East Siberian Sea. This suggests that low temperature constrains UCYN-A2 and its haptophyte host in some areas of the Pacific AO sector, which is consistent with the finding of the highest growth rates of cultivated *B. bigelowii* and UCYN-A2 at 10–22°C (Mak et al., 2025). Similarly, at temperatures of 8–15°C, high abundances of UCYN-A2 have previously been found in the Bering Sea (Shiozaki et al., 2017) and were linked to high iron levels due to river runoff (Cheung et al., 2022). Unfortunately, iron was not measured in our study. However, the high abundance and activity of UCYN-A2 across all stations along the Alaskan Coast show that *B. bigelowii* and UCYN-A2 thrive here.

Our sequence data revealed elevated relative abundances and expression of NCDs, particularly at the low temperature and productivity stations at the Chukchi Plateau and in the East Siberian Sea (e.g., 29, 30, 31, 35, and 36; Figures 5a and 5b). This may merely reflect the decrease in UCYN-A abundance but indicates that NCDs were expressing *nifH* and likely fixing N_2. Interestingly, the Gammaproteobacterial genus *Tolumonas* sp. dominated the community composition at station 35 (98%). Stations 35 and 36 (East Siberian Sea) were situated close to the sea ice edge (~12 km; NOAA Ice Charts), and this genus has previously been found associated with land-fast ice (von Friesen, Farnelid, et al., 2025). Most NCDs belonged to Deltaproteobacteria (subclusters 3E and 1A) and were similar to NCDs previously found in the AO (Figure S2 in Supporting Information S1; Fernández-Méndez et al., 2016; Shiozaki et al., 2018; von Friesen, Farnelid, et al., 2025, von Friesen, Laber, et al., 2025). Hence, NCDs appear to play a role in Arctic N_2 fixation, particularly at the more northern, non-coastal stations. The reason for this distribution is unknown, but we note that river influenced shelf waters transported toward the center of the AO basin contain surprisingly high concentrations of iron complexed by organic matter (Charette et al., 2020). Moreover, melting sea ice may release substantial amounts of autochthonous DOM (Retelletti Brogi et al., 2018). Given the metabolic versality of NCDs and their ability to degrade "refractory" DOM (e.g., Bentzon-Tilia et al., 2015; Deng et al., 2025; Shiozaki et al., 2023), we speculate that this DOM benefits NCD diazotrophy by supplying both energy and iron.

N_2 fixation occurred throughout most of the Pacific sector of the AO, including the East Siberian Sea and Chukchi Plateau, where N_2 fixation, to our knowledge, has not been measured previously. Generally, rates were low (<1 nmol N L^{-1} d^{-1}), which is consistent with earlier data from the Pacific AO (Shiozaki et al., 2018), the central AO (von Friesen, Farnelid, et al., 2025), the Fram Strait (Zander, von Friesen, Gonçalves-Araujo, et al., 2026), and the Canadian Arctic (Blais et al., 2012). Hence, low N_2 fixation is widely distributed in the AO. Although many rates are close to the detection limit, they might still play an important role in N cycling and productivity due to the prevailing low DIN concentrations across the AO in summer. Indeed, although the potential contribution of nitrogen fixation to primary production was generally below 1%, it was much higher, up to 16%, in discrete samples (Table S3 in Supporting Information S1). Such high variability between samples has been observed earlier elsewhere (e.g., Hallstrøm, Benavides, et al., 2022; von Friesen, Farnelid, et al., 2025, von Friesen, Laber, et al., 2025) but remains unexplained to our knowledge.

Identifying environmental drivers of N_2 fixation is challenging, as they vary across regions and likely involve multiple interacting factors, such as for example temperature, nutrient availability, productivity, and trophic controls (Zehr & Capone, 2021). Here, we observed a tendency to lower N_2 fixation and primary production in the low temperature waters north of the Chukchi Sea, accompanied by decreased bacterial abundances and chl. *a* concentrations. For example, temperature at stations 29, 31, 35, and 36 (5 m) was <0°C, and at three of these

21698961, 2026, 10, Downloaded from https://agupubs.onlinelibrary.wiley.com/doi/10.1029/2026JG009929 by Statens Beredning, Wiley Online Library on [30/10/2026]. See the Terms and Conditions (https://onlinelibrary.wiley.com/terms-and-conditions) on Wiley Online Library for rules of use; OA articles are governed by the applicable Creative Commons License

stations, N_2 fixation was below LOD, and primary production was the lowest measured throughout the cruise. Hence, low productivity and temperature may constrain N_2 fixation in this region. Overall, we found no statistical linkage between N_2 fixation and DOM characteristics, that is, the relative allochthonous and autochthonous DOM influence, but we note that N_2 fixation was stimulated by amendment with phytoplankton-derived compounds at station 36 (see above). Taken together, we speculate that N_2 fixation occurs primarily in waters above a threshold in bacterio- and phytoplankton productivity and, thereby, in bioavailable DOM. However, statistical identification of drivers of N_2 fixation is likely hampered by their heterogeneous spatial distribution, particularly in studies involving different water masses, such as ours.

5. Concluding Remarks and Perspectives

Our study shows that N_2 fixation is low but widespread in the Pacific AO across areas with contrasting environmental conditions and DOM characteristics. Experimental amendments with bioavailable and a terrestrial DOM proxy showed stimulation of UCYN-A (and likely its haptophyte host), and occasionally N_2 fixation rates. Climate change is predicted to cause elevated primary production (Arrigo & van Dijken, 2015; Lewis et al., 2020) and increased nitrogen limitation (Tuerena et al., 2022) in the AO, driven in part by intensifying benthic denitrification on the Chukchi and East Siberian shelves as sea ice loss increases shelf primary production (Santos-García et al., 2026). Based on our study, the concomitant elevated riverine inflow of terrestrial DOM (Kong et al., 2025) and the increased availability of phytoplankton-derived compounds associated with the elevated phytoplankton biomass (Baines & Pace, 1991) may stimulate N_2 fixation locally in the future Pacific AO. However, given the limited and spatially variable experimental evidence provided here, we recommend additional work to decipher the influence of allochthonous and autochthonous DOM on N_2 fixation in the AO. Determining the rates and spatial variability of N_2 fixation will be instrumental for predicting future primary production and food web structure in this important ocean.

Conflict of Interest

The authors declare no conflicts of interest relevant to this study.

Availability Statement

Sequences are deposited in the National Centre for Biotechnology Information (NCBI) Sequence Read Archive under reference number PRJNA1438606. Data tables for ASV counts, taxonomy, and sequences in FASTA format along with scripts and data for correlation analyses can be found in Zander, von Friesen, Fujiwara, et al. (2026).

Acknowledgments

We thank the captain and crew of R/V *Mirai* and Mariko Hatta for coordinating the CTD sampling. We also thank Cecilie Fryland Appeldorff, Sara Lykke Brinch, and Jeanett Hansen for laboratory assistance. Finally, we thank five anonymous reviewers for their helpful comments on the manuscript. This work was supported by the Independent Research Fund Denmark [2032-00001B] to LR, CAS, and TS. The Danish National Research Foundation supported activities within the Center for Volatile Interactions (DNFR168). MB was supported by the BIOPOLE National Capability Multicentre Round 2 funding from the Natural Environment Research Council (NE/W004933/1). AF and TS were supported by the Arctic Challenge for Sustainability II and III (ArCS II and III) from the Japanese Ministry of Education, Culture, Sports, Science and Technology (MEXT). Field work was supported via the early career scientist call through ArCS II (Japan Agency for Marine-Earth Science and Technology) and the Ymer-80 foundation for young polar researchers to LWvF.

References

Amon, R. M. W., & Meon, B. (2004). The biogeochemistry of dissolved organic matter and nutrients in two large Arctic estuaries and potential implications for our understanding of the Arctic Ocean system. *Marine Chemistry*, *92*(1–4), 311–330. https://doi.org/10.1016/j.marchem.2004.06.034

Angel, R., Nepel, M., Panhölzl, C., Schmidt, H., Herbold, C. W., Eichorst, S. A., & Woebken, D. (2018). Evaluation of primers targeting the diazotroph functional gene and development of NifMAP—A bioinformatics pipeline for analyzing *nifH* amplicon data. *Frontiers in Microbiology*, *9*, 703. https://doi.org/10.3389/fmicb.2018.00703

Ardyna, M., & Arrigo, K. R. (2020). Phytoplankton dynamics in a changing Arctic Ocean. *Nature Climate Change*, *10*, 892–903. https://doi.org/10.1038/s41558-020-0905-y

Armbruster, D. A., & Pry, T. (2008). Limit of blank, limit of detection and limit of quantitation. *Clinical Biochemist Reviews*, *29*, 49–52.

Arrigo, K. R., & van Dijken, G. L. (2015). Continued increases in Arctic Ocean primary production. *Progress in Oceanography*, *136*, 60–70. https://doi.org/10.1016/j.pocean.2015.05.002

Baines, S. B., & Pace, M. L. (1991). The production of dissolved organic matter by phytoplankton and its importance to bacteria: Patterns across marine and freshwater systems. *Limnology and Oceanography*, *36*(6), 1078–1090. https://doi.org/10.4319/lo.1991.36.6.1078

Barnett, D., Arts, I., & Penders, J. (2021). microViz: An R package for microbiome data visualization and statistics. *Journal of Open Source Software*, *6*(63), 3201. https://doi.org/10.21105/joss.03201

Bates, N. R., & Mathis, J. T. (2009). The Arctic Ocean marine carbon cycle: Evaluation of air-sea CO_2 exchanges, ocean acidification impacts and potential feedbacks. *Biogeosciences Discussions*, *6*(11), 2433–2459. https://doi.org/10.5194/bg-6-2433-2009

Benavides, M., Berthelot, H., Duhamel, S., Raimbault, P., & Bonnet, S. (2017). Dissolved organic matter uptake by *Trichodesmium* in the Southwest Pacific. *Scientific Reports*, *7*(1), 41315. https://doi.org/10.1038/srep41315

Benavides, M., Bonnet, S., Hernández, N., Martínez-Pérez, A. M., Nieto-Cid, M., Álvarez-Salgado, X. A., et al. (2016). Basin-wide N_2 fixation in the deep waters of the Mediterranean Sea. *Global Biogeochemical Cycles*, *30*(6), 952–961. https://doi.org/10.1002/2015GB005326

Benavides, M., Bonnet, S., Le Moigne, F. A. C., Armin, G., Inomura, K., Hallstrøm, S., et al. (2022). Sinking *Trichodesmium* fixes nitrogen in the dark ocean. *ISME Journal*, *16*(10), 2398–2405. https://doi.org/10.1038/s41396-022-01289-6

Benavides, M., Duhamel, S., Van Wambeke, F., Shoemaker, K. M., Moisander, P. H., Salamon, E., et al. (2020). Dissolved organic matter stimulates N_2 fixation and *nifH* gene expression in *Trichodesmium*. *FEMS Microbiology Letters*, *367*(4), fnaa034. https://doi.org/10.1093/femsle/fnaa034

Benavides, M., Moisander, P. H., Berthelot, H., Dittmar, T., Grosso, O., & Bonnet, S. (2015). Mesopelagic N_2 fixation related to organic matter composition in the Solomon and Bismarck Seas (Southwest Pacific). *PLoS One*, *10*(12), e0143775. https://doi.org/10.1371/journal.pone.0143775

Benner, R., Louchouarn, P., & Amon, R. M. W. (2005). Terrigenous dissolved organic matter in the Arctic Ocean and its transport to surface and deep waters of the North Atlantic. *Global Biogeochemical Cycles*, *19*(2), 2004GB002398. https://doi.org/10.1029/2004GB002398

Bentzon-Tilia, M., Severin, I., Hansen, L. H., & Riemann, L. (2015). Genomics and ecophysiology of heterotrophic nitrogen-fixing bacteria isolated from estuarine surface water. *mBio*, *6*(4), e00929-15. https://doi.org/10.1128/mBio.00929-15

Blais, M., Tremblay, J., Jungblut, A. D., Gagnon, J., Martin, J., Thaler, M., & Lovejoy, C. (2012). Nitrogen fixation and identification of potential diazotrophs in the Canadian Arctic. *Global Biogeochemical Cycles*, *26*(3), 2011GB004096. https://doi.org/10.1029/2011GB004096

Bombar, D., Paerl, R. W., & Riemann, L. (2016). Marine non-cyanobacterial diazotrophs: Moving beyond molecular detection. *Trends in Microbiology*, *24*(11), 916–927. https://doi.org/10.1016/j.tim.2016.07.002

Bonnet, S., Dekaezemacker, J., Turk-Kubo, K. A., Moutin, T., Hamersley, R. M., Grosso, O., et al. (2013). Aphotic N_2 fixation in the eastern tropical South Pacific Ocean. *PLoS One*, *8*(12), e81265. https://doi.org/10.1371/journal.pone.0081265

Callahan, B. J., McMurdie, P. J., Rosen, M. J., Han, A. W., Johnson, A. J. A., & Holmes, S. P. (2016). DADA2: High-resolution sample inference from illumina amplicon data. *Nature Methods*, *13*(7), 581–583. https://doi.org/10.1038/nmeth.3869

Capone, D. G., Burns, J. A., Montoya, J. P., Subramaniam, A., Mahaffey, C., Gunderson, T., et al. (2005). Nitrogen fixation by *Trichodesmium* spp.: An important source of new nitrogen to the tropical and subtropical North Atlantic Ocean. *Global Biogeochemical Cycles*, *19*(2), GB2024. https://doi.org/10.1029/2004gb002331

Chakraborty, S., Andersen, K. H., Visser, A. W., Inomura, K., Follows, M. J., & Riemann, L. (2021). Quantifying nitrogen fixation by heterotrophic bacteria in sinking marine particles. *Nature Communications*, *12*(1), 4085. https://doi.org/10.1038/s41467-021-23875-6

Charette, M. A., Kipp, L. E., Jensen, L. T., Dabrowski, J. S., Whitmore, L. M., Fitzsimmons, J. N., et al. (2020). The transpolar drift as a source of riverine and shelf-derived trace elements to the central Arctic Ocean. *Journal of Geophysical Research: Oceans*, *125*(5), e2019JC015920. https://doi.org/10.1029/2019JC015920

Cheung, S., Liu, K., Turk-Kubo, K. A., Nishioka, J., Suzuki, K., Landry, M. R., et al. (2022). High biomass turnover rates of endosymbiotic nitrogen-fixing cyanobacteria in the western Bering Sea. *Limnology and Oceanography Letters*, *7*(6), 501–509. https://doi.org/10.1002/lol2.10267

Church, M., Jenkins, B., Karl, D., & Zehr, J. (2005). Vertical distributions of nitrogen-fixing phylotypes at Stn Aloha in the oligotrophic North Pacific Ocean. *Aquatic Microbial Ecology*, *38*, 3–14. https://doi.org/10.3354/ame038003

Coale, T. H., Loconte, V., Turk-Kubo, K. A., Vanslembrouck, B., Mak, W. K. E., Cheung, S., et al. (2024). Nitrogen-fixing organelle in a marine alga. *Science*, *384*(6692), 217–222. https://doi.org/10.1126/science.adk1075

Dainard, P. G., & Guéguen, C. (2013). Distribution of PARAFAC modeled CDOM components in the North Pacific Ocean, Bering, Chukchi and Beaufort Seas. *Marine Chemistry*, *157*, 216–223. https://doi.org/10.1016/j.marchem.2013.10.007

Davis, N. M., Proctor, D. M., Holmes, S. P., Relman, D. A., & Callahan, B. J. (2018). Simple statistical identification and removal of contaminant sequences in marker-gene and metagenomics data. *Microbiome*, *6*(1), 226. https://doi.org/10.1186/s40168-018-0605-2

Deng, L., Chen, J., Xu, Z., Lee, S. S., Cheung, S., & Liu, H. (2025). Global marine metagenomics reveals the functional diversity and ecological adaptations of diazotrophs across marine ecosystems. *Communications Earth & Environment*, *6*(1), 933. https://doi.org/10.1038/s43247-025-02850-9

Edler, D., Klein, J., Antonelli, A., & Silvestro, D. (2021). raxmlGUI 2.0: A graphical interface and toolkit for phylogenetic analyses using RAxML. *Methods in Ecology and Evolution*, *12*(2), 373–377. https://doi.org/10.1111/2041-210x.13512

Fernández-Méndez, M., Turk-Kubo, K. A., Buttigieg, P. L., Rapp, J. Z., Krumpen, T., Zehr, J. P., & Boetius, A. (2016). Diazotroph diversity in the sea ice, melt ponds, and surface waters of the Eurasian Basin of the Central Arctic Ocean. *Frontiers in Microbiology*, *7*, 1884. https://doi.org/10.3389/fmicb.2016.01884

Figueroa, D., Capo, E., Lindh, M. V., Rowe, O. F., Paczkowska, J., Pinhassi, J., & Andersson, A. (2021). Terrestrial dissolved organic matter inflow drives temporal dynamics of the bacterial community of a subarctic estuary (Northern Baltic Sea). *Environmental Microbiology*, *23*(8), 4200–4213. https://doi.org/10.1111/1462-2920.15597

Filella, A., Cébron, A., Paix, B., Vallet, M., Martinot, P., Guyomarch, L., et al. (2025). Organic metabolite uptake by diazotrophs in the North Pacific Ocean. *ISME Communications*, *5*(1), ycaf061. https://doi.org/10.1093/ismeco/ycaf061

Filella, A., Umbricht, J., Klett, A., Vogts, A., Vannier, T., Grosso, O., et al. (2024). Dissolved organic matter offsets the detrimental effects of climate change in the nitrogen-fixing cyanobacterium *Crocosphaera*. *Limnology and Oceanography Letters*, *9*(3), 296–306. https://doi.org/10.1002/lol2.10380

Frank, I. E., Turk-Kubo, K. A., & Zehr, J. P. (2016). Rapid annotation of *nifH* gene sequences using classification and regression trees facilitates environmental functional gene analysis. *Environmental Microbiology Reports*, *8*(5), 905–916. https://doi.org/10.1111/1758-2229.12455

Givati, S., Forchielli, E., Aharonovich, D., Barak, N., Weissberg, O., Belkin, N., et al. (2024). Diversity in the utilization of different molecular classes of dissolved organic matter by heterotrophic marine bacteria. *Applied and Environmental Microbiology*, *90*(7), e00256-24. https://doi.org/10.1128/aem.00256-24

Gradoville, M. R., Bombar, D., Crump, B. C., Letelier, R. M., Zehr, J. P., & White, A. E. (2017). Diversity and activity of nitrogen-fixing communities across ocean basins. *Limnology and Oceanography*, *62*(5), 1895–1909. https://doi.org/10.1002/lno.10542

Gradoville, M. R., Cabello, A. M., Wilson, S. T., Turk-Kubo, K. A., Karl, D. M., & Zehr, J. P. (2021). Light and depth dependency of nitrogen fixation by the non-photosynthetic, symbiotic cyanobacterium UCYN-A. *Environmental Microbiology*, *23*(8), 4518–4531. https://doi.org/10.1111/1462-2920.15645

Grieman, M. M., Aydin, M., Isaksson, E., Schwikowski, M., & Saltzman, E. S. (2018). Aromatic acids in an Arctic ice core from Svalbard: A proxy record of biomass burning. *Climate of the Past*, *14*(5), 637–651. https://doi.org/10.5194/cp-14-637-2018

Grunert, B. K., Tzortziou, M., Neale, P., Menendez, A., & Hernes, P. (2021). DOM degradation by light and microbes along the Yukon River-coastal ocean continuum. *Scientific Reports*, *11*(1), 10236. https://doi.org/10.1038/s41598-021-89327-9

Hagino, K., Onuma, R., Kawachi, M., & Horiguchi, T. (2013). Discovery of an endosymbiotic nitrogen-fixing cyanobacterium UCYN-A in *Braarudosphaera bigelowii* (Prymnesiophyceae). *PLoS One*, *8*(12), e81749. https://doi.org/10.1371/journal.pone.0081749

Hallstrøm, S., Benavides, M., Salamon, E. R., Arístegui, J., & Riemann, L. (2022). Activity and distribution of diazotrophic communities across the Cape Verde Frontal Zone in the Northeast Atlantic Ocean. *Biogeochemistry*, *160*(1), 49–67. https://doi.org/10.1007/s10533-022-00940-w

21698961, 2026, 10, Downloaded from https://agupubs.onlinelibrary.wiley.com/doi/10.1029/2026JG009929 by Statens Beredning, Wiley Online Library on [30/10/2026]. See the Terms and Conditions (https://onlinelibrary.wiley.com/terms-and-conditions) on Wiley Online Library for rules of use; OA articles are governed by the applicable Creative Commons License

Hallstrøm, S., Raina, J.-B., Ostrowski, M., Parks, D. H., Tyson, G. W., Hugenholtz, P., et al. (2022). Chemotaxis may assist marine heterotrophic bacterial diazotrophs to find microzones suitable for N_2 fixation in the pelagic ocean. *ISME Journal*, *16*(11), 2525–2534. https://doi.org/10.1038/s41396-022-01299-4

Hama, T., Hama, J., & Handa, N. (1993). ^{13}C tracer methodology in microbial ecology with special reference to primary production processes in aquatic environments. *Advances in Microbial Ecology*, *13*, 39–83. https://doi.org/10.1007/978-1-4615-2858-6_2

Hansell, D. A., Kadko, D., & Bates, N. R. (2004). Degradation of terrigenous dissolved organic carbon in the western Arctic Ocean. *Science*, *304*(5672), 858–861. https://doi.org/10.1126/science.1096175

Harding, K., Turk-Kubo, K. A., Sipler, R. E., Mills, M. M., Bronk, D. A., & Zehr, J. P. (2018). Symbiotic unicellular cyanobacteria fix nitrogen in the Arctic Ocean. *Proceedings of the National Academy of Sciences*, *115*(52), 13371–13375. https://doi.org/10.1073/pnas.1813658115

Helms, J. R., Stubbins, A., Ritchie, J. D., Minor, E. C., Kieber, D. J., & Mopper, K. (2008). Absorption spectral slopes and slope ratios as indicators of molecular weight, source, and photobleaching of chromophoric dissolved organic matter. *Limnology and Oceanography*, *53*(3), 955–969. https://doi.org/10.4319/lo.2008.53.3.0955

Holmes, R. M., McClelland, J. W., Raymond, P. A., Frazer, B. B., Peterson, B. J., & Stieglitz, M. (2008). Lability of DOC transported by Alaskan rivers to the Arctic Ocean. *Geophysical Research Letters*, *35*(3), 2007GL032837. https://doi.org/10.1029/2007GL032837

JAMSTEC. (2023). R/V MIRAI MR23-06C Cruise data. https://doi.org/10.17596/0003983

Jørgensen, L., Stedmon, C. A., Kaartokallio, H., Middelboe, M., & Thomas, D. N. (2015). Changes in the composition and bioavailability of dissolved organic matter during sea ice formation. *Limnology and Oceanography*, *60*(3), 817–830. https://doi.org/10.1002/lno.10058

Kaiser, K., Benner, R., & Amon, R. M. W. (2017). The fate of terrigenous dissolved organic carbon on the Eurasian shelves and export to the North Atlantic. *Journal of Geophysical Research: Oceans*, *122*(1), 4–22. https://doi.org/10.1002/2016JC012380

Kana, T. M., Darkangelo, C., Hunt, M. D., Oldham, J. B., Bennett, G. E., & Cornwell, J. C. (1994). Membrane inlet mass spectrometer for rapid high-precision determination of N_2, O_2, and Ar in environmental water samples. *Analytical Chemistry*, *66*(23), 4166–4170. https://doi.org/10.1021/ac00095a009

Katoh, K., & Standley, D. M. (2013). MAFFT multiple sequence alignment software version 7: Improvements in performance and usability. *Molecular Biology and Evolution*, *30*(4), 772–780. https://doi.org/10.1093/molbev/mst010

Klawonn, I., Lavik, G., Böning, P., Marchant, H. K., Dekaezemacker, J., Mohr, W., & Ploug, H. (2015). Simple approach for the preparation of $^{15-15}N_2$-enriched water for nitrogen fixation assessments: Evaluation, application and recommendations. *Frontiers in Microbiology*, *6*, 769. https://doi.org/10.3389/fmicb.2015.00769

Kong, X., Lechtenfeld, O. J., Kaesler, J. M., Granskog, M. A., Stedmon, C. A., Graeve, M., & Koch, B. P. (2025). Major terrestrial contribution to the dissolved organic carbon budget in the Arctic Ocean. *Nature Geoscience*, *19*(1), 90–98. https://doi.org/10.1038/s41561-025-01847-5

Kothawala, D. N., Murphy, K. R., Stedmon, C. A., Weyhenmeyer, G. A., & Tranvik, L. J. (2013). Inner filter correction of dissolved organic matter fluorescence. *Limnology and Oceanography: Methods*, *11*(12), 616–630. https://doi.org/10.4319/lom.2013.11.616

Kuzyk, Z. Z. A., Goñi, M. A., Stern, G. A., & Macdonald, R. W. (2008). Sources, pathways and sinks of particulate organic matter in Hudson Bay: Evidence from lignin distributions. *Marine Chemistry*, *112*(3–4), 215–229. https://doi.org/10.1016/j.marchem.2008.08.001

Letunic, I., & Bork, P. (2021). Interactive Tree Of Life (iTOL) v5: An online tool for phylogenetic tree display and annotation. *Nucleic Acids Research*, *49*(W1), W293–W296. https://doi.org/10.1093/nar/gkab301

Lewis, K. M., van Dijken, G. L., & Arrigo, K. R. (2020). Changes in phytoplankton concentration now drive increased Arctic Ocean primary production. *Science*, *369*(6500), 198–202. https://doi.org/10.1126/science.aay8380

Lu, P., Huang, H., Sun, Y., Qiang, M., Zhu, Y., Cao, M., et al. (2022). Biodegradation of 4-hydroxybenzoic acid by *Acinetobacter johnsonii* FZ-5 and *Klebsiella oxytoca* FZ-8 under anaerobic conditions. *Biodegradation*, *33*(1), 17–31. https://doi.org/10.1007/s10532-021-09963-w

Lu, P., Wang, W., Zhang, G., Li, W., Jiang, A., Cao, M., et al. (2020). Isolation and characterization marine bacteria capable of degrading lignin-derived compounds. *PLoS One*, *15*(10), e0240187. https://doi.org/10.1371/journal.pone.0240187

Mak, E. W. K., Turk-Kubo, K. A., Caron, D. A., Harbeitner, R. C., Magasin, J. D., Coale, T. H., et al. (2024). Phagotrophy in the nitrogen-fixing haptophyte *Braarudosphaera bigelowii*. *Environmental Microbiology Reports*, *16*, e13312. https://doi.org/10.1111/1758-2229.13312

Mak, E. W. K., Turk-Kubo, K. A., Voznyuk, A. V., Gradoville, M. R., Coale, T., Hagino, K., & Zehr, J. P. (2025). Temperature-dependent growth and activity in a globally distributed nitrogen-fixing haptophyte. *Limnology and Oceanography*, *70*(5), 1499–1511. https://doi.org/10.1002/lno.70050

Manizza, M., Menemenlis, D., Zhang, H., & Miller, C. E. (2019). Modeling the recent changes in the Arctic Ocean CO_2 Sink (2006–2013). *Global Biogeochemical Cycles*, *33*(3), 420–438. https://doi.org/10.1029/2018GB006070

Mann, P. J., Davydova, A., Zimov, N., Spencer, R. G. M., Davydov, S., Bulygina, E., et al. (2012). Controls on the composition and lability of dissolved organic matter in Siberia's Kolyma river basin. *Journal of Geophysical Research*, *117*(G1), G01028. https://doi.org/10.1029/2011JG001798

Mann, P. J., Spencer, R. G. M., Hernes, P. J., Six, J., Aiken, G. R., Tank, S. E., et al. (2016). Pan-Arctic trends in terrestrial dissolved organic matter from optical measurements. *Frontiers in Earth Science*, *4*, 25. https://doi.org/10.3389/feart.2016.00025

Martiny, A. C., Pham, C. T. A., Primeau, F. W., Vrugt, J. A., Moore, J. K., Levin, S. A., & Lomas, M. W. (2013). Strong latitudinal patterns in the elemental ratios of marine plankton and organic matter. *Nature Geoscience*, *6*(4), 279–283. https://doi.org/10.1038/ngeo1757

Mathew, S., Hong, J.-K., Kim, J.-H., Chen, M., & Hur, J. (2025). Terrestrial inputs of nutrients and dissolved organic carbon to the Arctic Ocean and their influence on primary production. *Marine Environmental Research*, *209*, 107182. https://doi.org/10.1016/j.marenvres.2025.107182

Mathis, J. T., Pickart, R. S., Hansell, D. A., Kadko, D., & Bates, N. R. (2007). Eddy transport of organic carbon and nutrients from the Chukchi Shelf: Impact on the upper halocline of the western Arctic Ocean. *Journal of Geophysical Research*, *112*(C5), 2006JC003899. https://doi.org/10.1029/2006JC003899

McClelland, J. W., Holmes, R. M., Dunton, K. H., & Macdonald, R. W. (2012). The Arctic Ocean Estuary. *Estuaries and Coasts*, *35*(2), 353–368. https://doi.org/10.1007/s12237-010-9357-3

McMurdie, P. J., & Holmes, S. (2013). phyloseq: An R package for reproducible interactive analysis and graphics of microbiome census data. *PLoS One*, *8*(4), e61217. https://doi.org/10.1371/journal.pone.0061217

Mills, M. M., Brown, Z. W., Laney, S. R., Ortega-Retuerta, E., Lowry, K. E., Van Dijken, G. L., & Arrigo, K. R. (2018). Nitrogen limitation of the summer phytoplankton and heterotrophic prokaryote communities in the Chukchi Sea. *Frontiers in Marine Science*, *5*, 362. https://doi.org/10.3389/fmars.2018.00362

Moisander, P. H., Zhang, R., Boyle, E. A., Hewson, I., Montoya, J. P., & Zehr, J. P. (2012). Analogous nutrient limitations in unicellular diazotrophs and *Prochlorococcus* in the South Pacific Ocean. *ISME Journal*, *6*(4), 733–744. https://doi.org/10.1038/ismej.2011.152

Moynihan, M. A., & Furbo Reeder, C. (2023). nifHdada2 Github repository [Dataset]. *Zenodo*, 7996213. https://doi.org/10.5281/zenodo.7996213

Ngugi, D. K., Tsanuo, M. K., & Boga, H. I. (2007). Benzoic acid-degrading bacteria from the intestinal tract of *Macrotermes michaelseni* Sjöstedt. *Journal of Basic Microbiology*, *47*(1), 87–92.

21698961, 2026, 10, Downloaded from https://agupubs.onlinelibrary.wiley.com/doi/10.1029/2026JG009929 by Statens Beredning, Wiley Online Library on [30/10/2026]. See the Terms and Conditions (https://onlinelibrary.wiley.com/terms-and-conditions) on Wiley Online Library for rules of use; OA articles are governed by the applicable Creative Commons License

Norris, N., Levine, N. M., Fernandez, V. I., & Stocker, R. (2021). Mechanistic model of nutrient uptake explains dichotomy between marine oligotrophic and copiotrophic bacteria. *PLoS Computational Biology*, *17*(5), e1009023. https://doi.org/10.1371/journal.pcbi.1009023

Oksanen, J., Simpson, G., Blanchet, F. G., Kindt, R., Legendre, P., Minchin, P., et al. (2022). Vegan community ecology package version 2.6-2 April 2022.

Opsahl, S., Benner, R., & Amon, R. (1999). Major flux of terrigenous dissolved organic matter through the Arctic Ocean. *Limnology and Oceanography*, *44*(8), 2017–2023. https://doi.org/10.4319/lo.1999.44.8.2017

Parlanti, E., Wörz, K., Geoffroy, L., & Lamotte, M. (2000). Dissolved organic matter fluorescence spectroscopy as a tool to estimate biological activity in a coastal zone submitted to anthropogenic inputs. *Organic Geochemistry*, *31*(12), 1765–1781. https://doi.org/10.1016/s0146-6380(00)00124-8

Rahav, E., Giannetto, M. J., & Bar-Zeev, E. (2016). Contribution of mono and polysaccharides to heterotrophic N_2 fixation at the eastern Mediterranean coastline. *Scientific Reports*, *6*(1), 27858. https://doi.org/10.1038/srep27858

Raina, J.-B., Lambert, B. S., Parks, D. H., Rinke, C., Siboni, N., Bramucci, A., et al. (2022). Chemotaxis shapes the microscale organization of the ocean's microbiome. *Nature*, *605*(7908), 132–138. https://doi.org/10.1038/s41586-022-04614-3

Rantanen, M., Karpechko, A. Y., Lipponen, A., Nordling, K., Hyvärinen, O., Ruosteenoja, K., et al. (2022). The Arctic has warmed nearly four times faster than the globe since 1979. *Communications Earth & Environment*, *3*(1), 168. https://doi.org/10.1038/s43247-022-00498-3

Redfield, A. C. (1934). *On the proportions of organic derivatives in sea water and their relation to the composition of plankton*. University Press of Liverpool.

Retelletti Brogi, S., Ha, S.-Y., Kim, K., Derrien, M., Lee, Y. K., & Hur, J. (2018). Optical and molecular characterization of dissolved organic matter (DOM) in the Arctic ice core and the underlying seawater (Cambridge Bay, Canada): Implication for increased autochthonous DOM during ice melting. *Science of the Total Environment*, *627*, 802–811. https://doi.org/10.1016/j.scitotenv.2018.01.251

Rudels, B., & Carmack, E. (2022). Arctic Ocean water mass structure and circulation. *Oceanography*, *35*, 52–65. https://doi.org/10.5670/oceanog.2022.116

Ryder, A. G., Stedmon, C. A., Harrit, N., & Bro, R. (2017). Calibration, standardization, and quantitative analysis of multidimensional fluorescence (MDF) measurements on complex mixtures (IUPAC Technical Report). *Pure and Applied Chemistry*, *89*(12), 1849–1870. https://doi.org/10.1515/pac-2017-0610

Santos-García, M., Ganeshram, R. J., Oziel, L., de Steur, L., Tuerena, R. E., & Stedmon, C. S. (2026). Sea ice loss drives a regime shift in Arctic Ocean nitrogen biogeochemistry. *Communications Earth & Environment*, *7*(1), 442. https://doi.org/10.1038/s43247-026-03569-x

Schlitzer, R. (2023). Ocean data view v.5.8.1. Retrieved from https://odv.awi.de

Severin, I., Bentzon-Tilia, M., Moisander, P. H., & Riemann, L. (2015). Nitrogenase expression in estuarine bacterioplankton influenced by organic carbon and availability of oxygen. *FEMS Microbiology Letters*, *362*(14), fnv105. https://doi.org/10.1093/femsle/fnv105

Shiozaki, T., Bombar, D., Riemann, L., Hashihama, F., Takeda, S., Yamaguchi, T., et al. (2017). Basin scale variability of active diazotrophs and nitrogen fixation in the North Pacific, from the tropics to the subarctic Bering Sea. *Global Biogeochemical Cycles*, *31*(6), 996–1009. https://doi.org/10.1002/2017GB005681

Shiozaki, T., Fujiwara, A., Ijichi, M., Harada, N., Nishino, S., Nishi, S., et al. (2018). Diazotroph community structure and the role of nitrogen fixation in the nitrogen cycle in the Chukchi Sea (western Arctic Ocean). *Limnology and Oceanography*, *63*(5), 2191–2205. https://doi.org/10.1002/lno.10933

Shiozaki, T., Nishimura, Y., Yoshizawa, S., Takami, H., Hamasaki, K., Fujiwara, A., et al. (2023). Distribution and survival strategies of endemic and cosmopolitan diazotrophs in the Arctic Ocean. *ISME Journal*, *17*(8), 1340–1350. https://doi.org/10.1038/s41396-023-01424-x

Sipler, R. E., Gong, D., Baer, S. E., Sanderson, M. P., Roberts, Q. N., Mulholland, M. R., & Bronk, D. A. (2017). Preliminary estimates of the contribution of Arctic nitrogen fixation to the global nitrogen budget. *Limnology and Oceanography Letters*, *2*(5), 159–166. https://doi.org/10.1002/lol2.10046

Sipler, R. E., Kellogg, C. T. E., Connelly, T. L., Roberts, Q. N., Yager, P. L., & Bronk, D. A. (2017). Microbial community response to terrestrially derived dissolved organic matter in the coastal Arctic. *Frontiers in Microbiology*, *8*, 1018. https://doi.org/10.3389/fmicb.2017.01018

Spencer, R. G. M., Aiken, G. R., Butler, K. D., Dornblaser, M. M., Striegl, R. G., & Hernes, P. J. (2009). Utilizing chromophoric dissolved organic matter measurements to derive export and reactivity of dissolved organic carbon exported to the Arctic Ocean: A case study of the Yukon River, Alaska. *Geophysical Research Letters*, *36*(6), 2008GL036831. https://doi.org/10.1029/2008GL036831

Stedmon, C. A., Amon, R. M. W., Bauch, D., Bracher, A., Gonçalves-Araujo, R., Hoppmann, M., et al. (2021). Insights into water mass origins in the central Arctic Ocean from in situ dissolved organic matter fluorescence. *Journal of Geophysical Research: Oceans*, *126*(7), e2021JC017407. https://doi.org/10.1029/2021JC017407

Stedmon, C. A., Amon, R. M. W., Rinehart, A. J., & Walker, S. A. (2011). The supply and characteristics of colored dissolved organic matter (CDOM) in the Arctic Ocean: Pan Arctic trends and differences. *Marine Chemistry*, *124*(1–4), 108–118. https://doi.org/10.1016/j.marchem.2010.12.007

Stedmon, C. A., & Markager, S. (2001). The optics of chromophoric dissolved organic matter (CDOM) in the Greenland Sea: An algorithm for differentiation between marine and terrestrially derived organic matter. *Limnology and Oceanography*, *46*(8), 2087–2093. https://doi.org/10.4319/lo.2001.46.8.2087

Tank, S. E., Manizza, M., Holmes, R. M., McClelland, J. W., & Peterson, B. J. (2012). The processing and impact of dissolved riverine nitrogen in the Arctic Ocean. *Eustaries Coasts*, *35*(2), 401–415. https://doi.org/10.1007/s12237-011-9417-3

Terhaar, J., Orr, J. C., Ethé, C., Regnier, P., & Bopp, L. (2019). Simulated Arctic Ocean response to doubling of riverine carbon and nutrient delivery. *Global Biogeochemical Cycles*, *33*(8), 1048–1070. https://doi.org/10.1029/2019GB006200

Thompson, A., Carter, B. J., Turk-Kubo, K., Malfatti, F., Azam, F., & Zehr, J. P. (2014). Genetic diversity of the unicellular nitrogen-fixing cyanobacteria UCYN-A and its prymnesiophyte host. *Environmental Microbiology*, *16*(10), 3238–3249. https://doi.org/10.1111/1462-2920.12490

Traving, S. J., Rowe, O., Jakobsen, N. M., Sørensen, H., Dinasquet, J., Stedmon, C. A., et al. (2017). The effect of increased loads of dissolved organic matter on estuarine microbial community composition and function. *Frontiers in Microbiology*, *8*. https://doi.org/10.3389/fmicb.2017.00351

Tremblay, J.-É., Anderson, L. G., Matrai, P., Coupel, P., Bélanger, S., Michel, C., & Reigstad, M. (2015). Global and regional drivers of nutrient supply, primary production and CO_2 drawdown in the changing Arctic Ocean. *Progress in Oceanography*, *139*, 171–196. https://doi.org/10.1016/j.pocean.2015.08.009

Tuerena, R. E., Mahaffey, C., Henley, S. F., De La Vega, C., Norman, L., Brand, T., et al. (2022). Nutrient pathways and their susceptibility to past and future change in the Eurasian Arctic Ocean. *Ambio*, *51*(2), 355–369. https://doi.org/10.1007/s13280-021-01673-0

21698961, 2026, 10, Downloaded from https://agupubs.onlinelibrary.wiley.com/doi/10.1029/2026JG009929 by Statens Beredning, Wiley Online Library on [30/10/2026]. See the Terms and Conditions (https://onlinelibrary.wiley.com/terms-and-conditions) on Wiley Online Library for rules of use; OA articles are governed by the applicable Creative Commons License

Turk-Kubo, K. A., Gradoville, M. R., Cheung, S., Cornejo-Castillo, F. M., Harding, K. J., Morando, M., et al. (2022). Non-cyanobacterial diazotrophs: Global diversity, distribution, ecophysiology, and activity in marine waters. *FEMS Microbiology Reviews*, *47*(6), fuac046. https://doi.org/10.1093/femsre/fuac046

von Friesen, L. W., Farnelid, H., von Appen, W.-J., Benavides, M., Grosso, O., Laber, C. P., et al. (2025). Nitrogen fixation under declining Arctic sea ice. *Communications Earth & Environment*, *6*(1), 811. https://doi.org/10.1038/s43247-025-02782-4

von Friesen, L. W., Laber, C. P., Kristensen, B. H., Nysted, E., Sundbom, M., Bertilsson, S., et al. (2025). From temperate to polar waters: Transition to non-cyanobacterial diazotrophy upon entering the Atlantic gateway of the Arctic Ocean. *Limnology and Oceanography*, *70*(10), 2924–2940. https://doi.org/10.1002/lno.70153

von Friesen, L. W., Paulsen, M. L., Müller, O., Gründger, F., & Riemann, L. (2023). Glacial meltwater and seasonality influence community composition of diazotrophs in Arctic coastal and open waters. *FEMS Microbiology Ecology*, *99*(8), fiad067. https://doi.org/10.1093/femsec/fiad067

von Friesen, L. W., & Riemann, L. (2020). Nitrogen fixation in a changing Arctic Ocean: An overlooked source of nitrogen? *Frontiers in Microbiology*, *11*, 596426. https://doi.org/10.3389/fmicb.2020.596426

von Jackowski, A., Grosse, J., Nöthig, E.-M., & Engel, A. (2020). Dynamics of organic matter and bacterial activity in the Fram Strait during summer and autumn. *Philosophical Transactions. Series A, Mathematical, Physical, and Engineering Sciences*, *378*(2181), 20190366. https://doi.org/10.1098/rsta.2019.0366

White, A. E., Granger, J., Selden, C., Gradoville, M. R., Potts, L., Bourbonnais, A., et al. (2020). A critical review of the $^{15}N_2$ tracer method to measure diazotrophic production in pelagic ecosystems. *Limnology and Oceanography: Methods*, *18*(4), 129–147. https://doi.org/10.1002/lom3.10353

Wickham, H. (2016). ggplot2. v.3.4.0. https://doi.org/10.1007/978-3-319-24277-4

Williford, T., Amon, R. M. W., Kaiser, K., Benner, R., Stedmon, C., Bauch, D., et al. (2022). Spatial complexity in dissolved organic matter and trace elements driven by hydrography and freshwater input across the Arctic Ocean during 2015 Arctic GEOTRACES expeditions. *Journal of Geophysical Research: Oceans*, *127*(11), e2022JC018917. https://doi.org/10.1029/2022JC018917

Woodgate, R. A., Weingartner, T. J., & Lindsay, R. (2012). Observed increases in Bering Strait oceanic fluxes from the Pacific to the Arctic from 2001 to 2011 and their impacts on the Arctic Ocean water column. *Geophysical Research Letters*, *39*(24), 2012GL054092. https://doi.org/10.1029/2012GL054092

Zander, S., von Friesen, L. W., Fujiwara, A., Wünsch, U., Grosso, O., Benavides, M., et al. (2026). Dissolved organic matter impacts nitrogen fixation in the Arctic Ocean. [Dataset]. *Zenodo*. https://doi.org/10.5281/zenodo.22029753

Zander, S., von Friesen, L. W., Gonçalves-Araujo, R., Grosso, O., Benavides, M., Granskog, M. A., & Riemann, L. (2026). Contrasting nitrogen fixation between Arctic and Atlantic waters in the Fram Strait. *Microbial Ecology*, *89*(1), 26. https://doi.org/10.1007/s00248-025-02673-3

Zani, S., Mellon, M. T., Collier, J. L., & Zehr, J. P. (2000). Expression of *nifH* genes in natural microbial assemblages in Lake George, New York, detected by reverse transcriptase PCR. *Applied and Environmental Microbiology*, *66*(7), 3119–3124. https://doi.org/10.1128/AEM.66.7.3119-3124.2000

Zehr, J. P., Bench, S. R., Carter, B. J., Hewson, I., Niazi, F., Shi, T., et al. (2008). Globally distributed uncultivated oceanic N_2 -fixing cyanobacteria lack oxygenic photosystem II. *Science*, *322*(5904), 1110–1112. https://doi.org/10.1126/science.1165340

Zehr, J. P., & Capone, D. G. (2021). Marine nitrogen fixation. https://doi.org/10.1007/978-3-030-67746-6

Zehr, J. P., & Capone, D. G. (2020). Changing perspectives in marine nitrogen fixation. *Science*, *368*(6492), eaay9514. https://doi.org/10.1126/science.aay9514

Zehr, J. P., & McReynolds, L. A. (1989). Use of degenerate oligonucleotides for amplification of the nifH gene from the marine cyanobacterium *Trichodesmium thiebautii*. *Applied and Environmental Microbiology*, *55*(10), 2522–2526. https://doi.org/10.1128/aem.55.10.2522-2526.1989

Zehr, J. P., Mellon, M. T., & Zani, S. (1998). New nitrogen-fixing microorganisms detected in oligotrophic oceans by amplification of nitrogenase (*nifH*) genes. *Applied and Environmental Microbiology*, *64*(9), 3444–3450. https://doi.org/10.1128/AEM.64.9.3444-3450.1998

Zehr, J. P., & Turner, P. J. (2001). Nitrogen fixation: Nitrogenase genes and gene expression. In *Methods in microbiology* (pp. 271–286). Elsevier. https://doi.org/10.1016/S0580-9517(01)30049-1

References From the Supporting Information

Chien, Y. T., & Zinder, S. H. (1996). Cloning, functional organization, transcript studies, and phylogenetic analysis of the complete nitrogenase structural genes (nifHDK2) and associated genes in the archaeon *Methanosarcina barkeri* 227. *Journal of Bacteriology*, *178*(1), 143–148. https://doi.org/10.1128/jb.178.1.143-148.1996

21698961, 2026, 10, Downloaded from https://agupubs.onlinelibrary.wiley.com/doi/10.1029/2026JG009929 by Statens Beredning, Wiley Online Library on [30/10/2026]. See the Terms and Conditions (https://onlinelibrary.wiley.com/terms-and-conditions) on Wiley Online Library for rules of use; OA articles are governed by the applicable Creative Commons License